UC Irvine

UC Irvine Electronic Theses and Dissertations

Title

Electrochemical Immunosensors on Centrifugal Microfluidic Platforms

Permalink

https://escholarship.org/uc/item/0t51b1vc

Author

Bartoli Ramon, Jaume

Publication Date

2018

Peer reviewed|Thesis/dissertation

eScholarship.org Powered by the California Digital Library
University of California

UNIVERSITY OF CALIFORNIA,
IRVINE

Electrochemical Immunosensors on Centrifugal Microfluidic Platforms

THESIS

submitted in partial satisfaction of the requirements
for the degree of

MASTER OF SCIENCE

in Biomedical Engineering

by

Jaume Bartoli Ramon

Thesis Committee:
Professor Marc Madou, Chair
Professor William C. Tang
Professor Manuel Gamero-Castaño

2018

© 2018 Jaume Bartoli Ramon

TABLE OF CONTENTS

LIST OF FIGURES

LIST OF TABLES

ACKNOWLEDGEMENTS

I would like to thank Prof. Marc Madou for his guidance throughout the course of my MS research as well as for providing technical suggestions and valuable feedback on how to improve my thesis and research articles writing. I am also thankful to Maria Bauer with who I have been working closely to achieve the outcomes of this thesis. She introduced me to the field of electrochemical detection on centrifugal microfluidics, provided me with valuable insight into rapid prototyping techniques, and trained me to run electrochemical experiments. Finally, I would like to thank the Balsells Fellowship for its financial support.

ABSTRACT OF THE THESIS

Electrochemical Immunosensors on Centrifugal Microfluidic Platforms

By

Jaume Bartoli Ramon

Master of Science in Biomedical Engineering

University of California, Irvine, 2018

Professor Marc Madou, Chair

Here we present a fully integrated centrifugal microfluidic device that allows for automation of an enzyme-linked immunosorbent assay (ELISA), a common analytical biochemistry assay that would normally be performed either through labor-intensive and time-consuming protocols or by large and expensive analyzers. The system features a novel wireless readout approach that enables continuous, real-time electrochemical measurements with low levels of noise and high stability, even when the microfluidic disc is spinning at high velocities. Furthermore, redox cycling-amplified electrochemical detection is achieved by using interdigitated electrode arrays (IDEAs) as the sensing electrodes. We report that imposing flow over the electrodes by spinning the disc leads to improved sensor performance: a sensitivity of 6.99μA/mM and a limit of detection of 9.23nM are achieved at a slow flow rate of 203.4μL/min, which was demonstrated using the ferri-ferrocyanide redox-couple as the analyte solution. Prior to electrochemical detection, automated sample and reagent handling are achieved by designing a microfluidic system to release liquids sequentially, utilizing single-shot optofluidic valves that are actuated by a low power laser. High success rate of valve opening and fine tuning of spin

speed enabled completion of the required assay steps on the disc. As a model system, antibody against Plasmodium, a marker of malaria, was used as the target biomolecule for detection. Aside from automating the assay, the platform allowed for a 1.5-fold increase in sensitivity in comparison to the off-disc protocol, which is attributed to the enhanced mixing conditions and flow-enhanced mass transport that happen on the disc.

1. INTRODUCTION

Parameters such as glucose, electrolytes, proteins and lipids in blood provide valuable information about the condition of the human body. Blood-based diagnoses of diseases rely on blood tests that are typically carried out in clinical laboratories using large automated analyzers operated by highly trained staff. Even though these complex machines allow for high throughput analysis, patient´s blood needs to be transported from the sample collection site to a centralized laboratory. Point-of-care (POC) testing, i.e. performing medical tests at the patient´s bedside, has emerged as a new diagnostic approach that aims to decrease turnaround time for laboratory tests in order to offer more efficient, effective medical treatments and improved quality of medical care[1,2].

In accordance to the World Health Organization, POC diagnostics must meet a minimum of seven requirements that conform the ASSURED criteria: affordable, sensitive, specific, user-friendly, rapid and robust, equipment-free, and deliverable to end users[3]. As a fundamental technology capable of making possible the realization of devices with these characteristics, lab-on-a-chip (LOC) systems have attracted attention during the past few decades. LOC systems are based on a combination of miniaturized fluidics, electronics and mechanical components that allows automated bioassays to be implemented with decreased reagent use, shortened processing times, and increased abilities for parallel processing[1]. Nevertheless, LOC systems are limited in their ability to dispense and control the flow of multiple reagents, which hinders the deployment of fully integrated systems capable of handling real samples such as whole blood. In most cases, they require complex actuation

systems and fluidic handling solutions, increasing the complexity and decreasing the usability and robustness of the setup[2,4].

Lab-on-a-disc (LOD) systems, also known as centrifugal microfluidic devices, appear as an alternative. Being a subcategory of LOC devices, LOD systems incorporate the same advantages as chip-based systems, yet with their added value of simplicity. Centrifugal microfluidic platforms are particularly advantageous in POC applications because the control of multiple fluidic transports requires only a common spindle motor, eliminating the need for external pumps, tubes and connections. These devices consist in a microfluidic compact disc (CD) accommodating fluidic channels and chambers that is spun by the motor in order to apply a centrifugal force that pumps liquids along the radial channels. This enables a highly efficient fluid transportation without disturbing bubbles or residual volumes, multiplexing of several assays, and reduction of contamination risk thanks to the elimination of pumping and valving interfaces to the outside world. In addition, density-based sample separation, such as needed for blood processing, is inherently available[5]. Many different assays for in vitro diagnostics have already been automated on a LOD platform, such as DNA analysis, enzyme-linked immunosorbent assay (ELISA) and clinical chemistry assays[6,7].

In order to realize automated analytical processes, two major functionalities need to be integrated on the microfluidic CD: liquid handling and analyte detection. As far as the first one, a microfluidic disc must be capable of performing operations such as aliquoting, volume metering and fluid mixing, similarly to those operations that would be performed using a pipette in a manual diagnostic assay. These operations require a highly controlled

routing of the fluids through the physical chambers and channels of the disc, which is achieved using valves. Effective valving technologies are therefore an essential component of the system, allowing for not only control of liquid movement but also isolation between the sample and the rest of the system in order to prevent unintended reactions. Valving techniques on centrifugal microfluidics can be either passive or active. Passive valves are actuated by the rotation of the disc, exploiting the surface tension and centrifugal force between the channel and the fluid. Despite its simplicity and cost-effectivity, passive valving has a limited reliability since the lack of a physical barrier can cause leakage of vapor or fluid into an unwanted area. Furthermore, variations in the local surface properties of the microchannels can cause changes in the velocity-dependent actuation of the valves, thus making difficult to implement relievable protocols. Active valves eliminate these shortcomings because they are independent of the centrifugal force and are actuated by external mechanisms instead. Examples of external actuators include heat sources, lasers and magnets. Despite the associated increase in complexity and cost, active valves provide higher reliability and robustness, and they are often required in multistep assays where complex fluidic design cannot be controlled only by tuning the motor spin speed[8].

Regarding analyte detection, various detection methods have been employed on CD microfluidic platforms, usually based on optical techniques such as absorbance, fluorescence, and chemiluminescence detection. Optical methods do not require direct connection of the spinning CD to a stationary power supply, thus providing a straightforward and contact-free detection approach. Despite this advantage, most commercial absorbance-based systems are not suitable for miniaturization and require rather thick discs (>10mm), due to the fact that the absorbance of the solution is

proportional to the optical path length. As far as fluorescence and luminescence-based systems, they do not depend on the optical path length of the sample, contributing to an increased sensitivity but at cost of complexity and size of instrumentation[9,10]. Electrochemical detection appears as an attractive alternative to optical detection because of its low cost, small equipment footprint, high sensitivity, specificity and portability[5]. Unlike optical approaches, this technique is feasible in turbid solutions, independent from optical path length, and does not require neither optical grade materials nor peripheral equipment with high electrical power demands[9]. Furthermore, the recent advances in the microfabrication of electrodes have made improved electrochemical measurements possible: microelectrodes allow for lower ohmic drop, reduced capacitance and enhanced mass transport, leading to increased sensitivity and shorter response times[9,10]. One arrangement of microelectrodes is that of the interdigitated electrode arrays (IDEAs) in which electroactive redox species cycle multiple times between two closely spaced electrodes before diffusing out into the bulk solution, resulting in an amplified signal and a lower limit of detection (LOD).

By using the aforementioned tools, this thesis is aimed at developing a fully integrated lab-on-a-disc system that carries out an automated immunoassay. Immunoassays are an indispensable tool in clinical diagnostics to detect and quantify concentrations of antibody or antigen in biological samples, which is needed to diagnose a variety of types of diseases such as cancers, heart diseases and infectious diseases. The enzyme-linked immune-sorbent assay (ELISA) is a specific form of immunoassay that provides high sensitivity, specificity, precision and throughput. It has been traditionally used for the diagnosis of diseases such as AIDS, malaria and hepatitis B. Even though ELISA and in a broader sense,

immunoassays, have been successfully performed in laboratory, they require labor-intensive and time-consuming protocols involving multiple steps of incubation and washing that often result in errors and inconsistent results[11]. As an alternative, automated systems are already available, but they are large and expensive[12]. Thus, diagnosis of diseases requiring an immunoassay would greatly benefit from a centrifugal microfluidic platform performing real time and fully automated sample testing at the bedside, with decreased costs and ensuring consistent results. The methodology taken in this thesis is based on the use of active valves and electrochemical detection, due to their superior capabilities in comparison to passive valves and optical detection respectively. In order to achieve the overall goal, this thesis works towards the completion of the following milestones:

- 1. Integration of electrochemical detection on a spinning disc.
- 2. Study of the effect of flow on electrochemical sensor performance.
- 3. Development of a microfluidic disc capable of running a commercial ELISA assay for the detection of antibodies against Plasmodium for malaria diagnostics.

2. BACKGROUND

The following section reviews previous research conducted in the area of centrifugal microfluidics for in vitro diagnostics, focusing on the different techniques that have been developed for fluidic handling and analyte detection. This review categorizes and describes these techniques, provides examples of diagnostic platforms employing them, and argues and proposes the solution that this thesis takes.

2.1 VALVING TECHNIQUES FOR FLUIDIC HANDLING

Passive Valves

Valving is one of the most essential functions in a microfluid CD. Moreover, it has a paramount importance in those more complex, multi-step assays where sequential dispensing of pre-stored reagents is required. As mentioned in the introduction, passive valves are neither reliable nor practical for the automation of this kind of assays. Capillary or burst valves, the most common type of passive valves, have the following limitations: they are not vapor-tight, the burst frequency (i.e. angular frequency at which the valve opens) is a dynamic property as the contact angle of polymer surfaces changes over time, and the disc needs to be sequentially rotated from low to high spin speed, not the reverse[13]. Other types of passive valves are hydrophobic, siphon and pneumatic valves. Even though they allow new possibilities for fluid routing, their actuation still depends on the angular velocity of the disc and therefore, they require fine tuning of the spin speed and their robustness is limited. Like capillary valves, they are also dependent on the contact angle, thus their actuation is sensitive to surface finish and manufacturing tolerances of the disc.

Despite these disadvantages, the simplicity and ease of fabrication of passive vales make them to remain advantageous. Lai et al., for example, demonstrated a fully integrated multiplexed ELISA for rat IgG on a CD in which fluid handling was achieved using only capillary valves. These valves had well-defined and well-separated burst frequencies, which was achieved by varying channel dimensions and the distance of the valve from the center of rotation[14].

Active Valves

As an alternative to passive valves, active valves can be implemented in a variety of ways with different degrees of complexity. The most commonly used active valves are paraffin wax valves. This is a phase-change valve consisting of a paraffin wax plug that bars the channel and that melts when activated by an infrared source. Park et al. demonstrated an improved version of this method by mixing the paraffin wax with iron oxide nanoparticles, creating the so-called laser irradiated ferrowax microvalves (LIFMs). This allowed for valve actuation via low-power lasers (1.5 W) and at a short response time (0.5 s), thus reducing exposure of the sample to excessive heat. By simply changing the designs of the ferrowax loading chamber and the position of the laser beam irradiation, microvalves could be actuated reversibly, which allows a simpler CD layout and a lower total number of valves[15]. Building on this technique, Lee et al. reported a fully integrated ELISA on a disc for detection of biomarkers of the Hepatitis B virus[12]. Other types of laser-actuated valves on a CD have also been described. For example, Garcia-Cordero et al. developed a single-use optofluidic valve consisting of a thin plastic sheet with a printed black dot towards which the optical energy from a laser is directed in order to create a localized heating that melts

an orifice in the plastic sheet. This creates a connection between two overlapping fluidic channels that were previously isolated by the sandwiched plastic sheet, as shown in Fig 1[16].

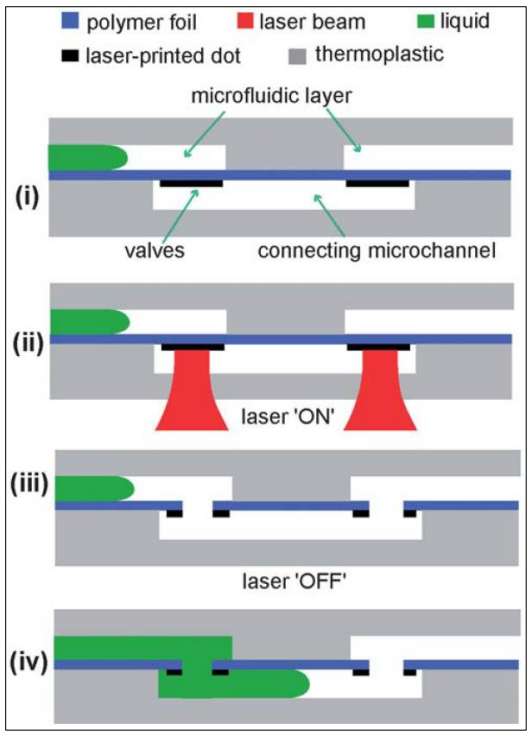

Fig. 1. Schematic of single-use laser valves. The operation sequence is as follows: (i) construction of the valves before piercing is shown; (ii) laser beams are pointed at the valves to pierce them; (iii) a path is open for liquid flow from the left (green); and (iv) liquid flows through the connecting channels. Note that the laser beam can be incident from either side of the device[16].

Aside from using heat sources, active valves can also be actuated pneumatically or magnetically. Pneumatic valves are typically actuated by expanding an air pocket. Abi-Samra et al., for example, used an infrared lamp to heat a ventless chamber of air, causing the air volume to expand and consequently, pushing out liquid from an adjacent chamber[17]. Noroozi et al. applied current to an electrolyte solution on the CD in order to generate electrolysis, which generated hydrogen and oxygen gas that pumped liquid out from the adjacent chamber[18], as shown in Fig. 2 (a). As far as magnetic valving, reversible actuation of valves is achieved by magnetically deforming a membrane. Haeberle et al., for example, created two valves each of them made by a steel plate integrated into a top PDMS layer of a CD which were actuated by a mounted external magnet when the plates passed over it,

causing pressurization of the gas in the chamber below the PDMS. Once the plates were no longer above the magnets, the valves opened, releasing the pressurized gas that was used to pump liquid from an adjacent chamber[19]. The functional principle is shown in Fig. 2 (b).

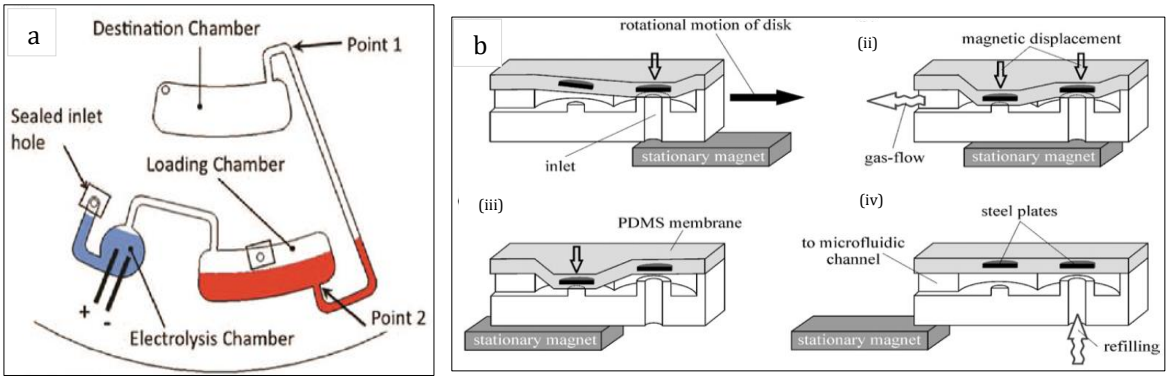

Fig. 2. Schematic of valving systems actuated pneumatically (a) and magnetically (b). Principles of operation are as follows. (a) When a current is sent through the electrolysis chamber (blue liquid), a gas is generated, pushing the liquid in the loading chamber (red) toward the destination chamber[18]. (b) The pump chamber orbits above a stationarity magnet and the two steel plates are spaced at a defined azimuthal distance, so that a sequence of displacements during rotation happen for pressurizing gas that is used to pump liquid from another chamber. After the magnet has passed, the chamber is refilled[19].

Semiactive Valves

In addition to active valves, semiactive valves can also be used to achieve a higher level of control compared to passive valves. Semiactive valves are also angular velocity-dependent, but they reduce the dependence on the reproducibility of the native surfaces of devices by integrating additional inexpensive materials, such as paper[5]. The most common semiactive valve is the dissolvable film (DF) valve. These valves breakdown when a liquid is introduced to their surface, eventually allowing liquid to pass through the valve. Gorkin et al. demonstrated a valving system combining DF valves and a pneumatic chamber. When the rotation speed reached a critical value, liquid could enter the pneumatic chamber, dissolve the DF, and pass into the downstream chamber (Fig. 3)[20].

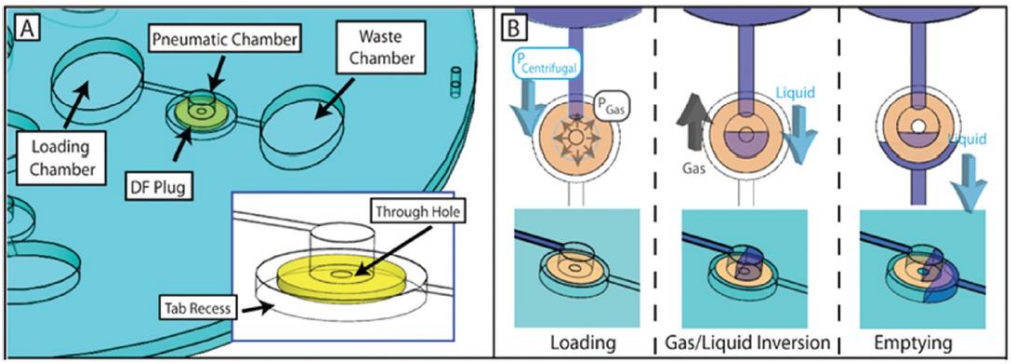

Fig. 3. Schematic of semiactive valving system using dissolvable films (DFs). (a) The design incorporates a pneumatic chamber before the DF as a barrier. Air is trapped in the pneumatic chamber before valve actuation. (b) At high spin speed, the liquid breaks into the pneumatic chamber and makes contact with the DF, which starts to dissolve. When the film is completely dissolved, the chamber empties[20].

Proposed Solution

A wide range of valving techniques with different degrees of reliability, complexity and cost are available. A balanced solution between these three aspects needs to be chosen, and further elements such as available materials and manufacturing techniques need to be taken into account in this decision. For the purposes of this thesis of implementing an ELISA on a CD, in which reliable flow control is crucial to ensure sequential dispensing of multiple reagents and isolation between them during the different assay steps, we choose active valves as the major valving technique. For their simple operation, the use of passive valves is not discarded. However, considering that the available manufacturing tolerances will smear the geometrically-defined burst frequencies of these valves into bands, only a very limited number of capillary valves could be used.

As far as the type of active valve, laser-actuated valves are considered in first place because of the simpler actuation mechanism that they employ in comparison to pneumatic and magnetic valves, where more complex fluidic layouts and external hardware is required. Finally, we incline towards the use of the single-use optofluidic valves developed by Garcia-

Cordero rather than the paraffin wax system. By only requiring a plastic sheet sandwiched between two layers of plastic containing the overlapping channels, the first system is simpler in design and materials. Moreover, unlike paraffin wax valves, this system is completely liquid- and vapor-tight. As far as its actuation, accuracy of the laser beam direction is less critical than in paraffin wax valves. Therefore, the solution proposed is to use a combination of capillary and optofluidic valves, with a predominance of the second ones because of their high utility and reliability.

2.2 ELECTROCHEMICAL TECHNIQUES FOR ANALYTE DETECTION

While some of the most widely used detection methods for bio assays are based on optical techniques, electrochemical detection attracts attention for its capability of being implemented in smaller, portable and lower cost diagnostic devices. Furthermore, as presented in the introduction, sensing using microelectrodes allows for lower limits of detection (LOD). While numerous potential biomarkers for disease diagnoses have been described, there is a lack of available diagnostic tests often due to the necessary but unreached LOD to reliably detect very low concentrations of proteins[21]. Therefore, due to the potential that electrochemical detection has to give rise to improved POCT diagnostics, this is a detection technique that is going to be considered in this thesis.

Amperometric Sensors

In biosensing, electrochemical detection extracts information from a biological sample by measuring an electronic signal which results from the transduction of a biological event. The most common type of electrochemical detection used in microfluidic systems is

amperometric detection. In amperometric detection, the current produced with either the reduction or oxidation of an electroactive species is monitored[5]. In order to generate the redox reaction, a suitable potential has to be applied between a working and a reference electrode. The resulting current is in direct proportion to the concentration of the target analyte. The most usual set up includes a third electrode, the counter, which allows the reference electrode to maintain a stable potential by acting as a source/sink of electrons to complete the electrical circuit. Different amperometric techniques are available depending on the potential that is applied to the working electrode. In chronoamperometry, a square-wave potential is applied, and the steady stated current is measured as a function of time. In voltammetry, the potential is varied form one fixed value to another. While there are many ways to vary this potential, cyclic voltammetry is one of the most widely used forms. In this case, the voltage is swept between two values at a fixed rate with a forward and backward scan. The scan rate is a critical factor because the duration of the scan must provide sufficient time to allow for a meaningful chemical reaction to occur[22]. Thus, different scan rates lead to different results. Both chronoamperometry and cyclic voltammetry are employed in this work.

Amperometric Microelectrodes

Mass transport of electroactive species from the bulk solution to the electrode surface is critical in electrochemical detection. Considering a static system (i.e. no convection) and with an increased ionic concentration (i.e. no migration), diffusion is the only form of mass transport. As introduced by Nerst, a diffusion layer grows on top of the electrode surface when a potential is applied. Upon application of the redox potential, the local analyte

concentration drops to zero at the electrode surface and a concentration gradient results, leading to the formation of the diffusion layer. In the bulk solution, the concentration of analyte is maintained. The use of microelectrodes allows for an improved mass transport through this diffusion layer. Microelectrodes have at least one dimension that is comparable to the diffusion layer thickness, which enables a converging mass diffusion flux. As opposed to the otherwise planar diffusion, radial diffusion allows for faster mass transport, which in turn leads to shorter response times and enhanced signal-to-noise ratio. Other advantages of microelectrodes are: high temporal and spatial resolution, measurements can be done in highly resistive media, and they can be used to analyze very small sample volumes[23].

Redox Cycling Amplification using Interdigitated Microelectrode Arrays

As a form of microelectrodes, interdigitated electrode arrays (IDEAs) offer not only the aforementioned advantages but also enhanced sensitivity and LOD through redox amplification. IDEAs use a 4-electrode setup in which two working electrodes are arranged in an interdigitated manner as seen in Fig. 4. Reduced species undergo oxidation at the electrode with the higher potential (generator), and oxidized species undergo reduction at the electrode with the lower potential (collector). This is referred as a dual mode measurement, as opposed to single mode measurement in which only one working electrode is employed. As the working principle of IDEAs, the sub-micrometer gap between the adjacent regions of the two electrodes causes the concentration gradients to overlap significantly, which allows the redox couple to redox cycle multiple times before diffusing out into the bulk solution[24]. This phenomenon is known as redox cycling, and it is

quantified using the collection efficiency (CE) parameter. Redox cycling generates higher currents, leading to the phenomenon known as redox amplification which is quantified using the redox amplification factor (RA) parameter. Generally, redox amplification has demonstrated to decrease the LOD through an increase in sensitivity. Odijik et al., for example, demonstrated an RA of over 2000 using a parallel plate setup with ferrocyanide as the redox-couple, and Dam et al. showed an RA of 60-70 with a high aspect ratio platinum IDAs with a width- gap- height of 2µm- 2µm- 7µm[25,26].

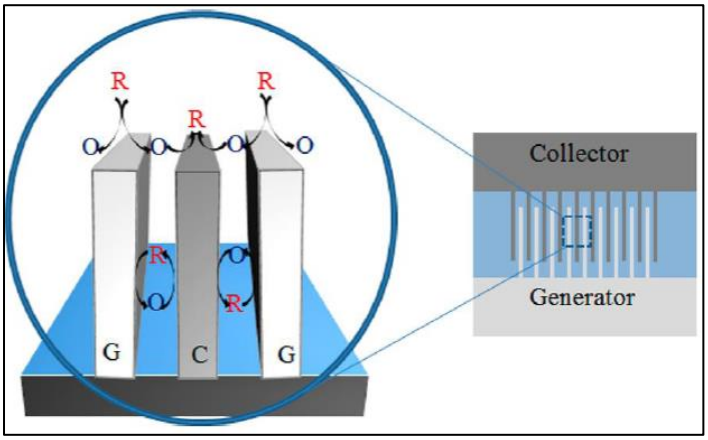

Fig. 4. Schematic of principle of redox cycling in a 3D IDEA. G: generator; C: collector[11].

Current Methods for Interfacing Electrochemical Detection on a Microfluidic CD

Due to the fact that the actuation principle in centrifugal microfluidics is based on a spinning disc, readout of the assay results poses a complex challenge. Optical detection offers the easiest solution due to the non-contact nature of the readout method, thus being by far the most widely used detection method in lab-on-a-disc platforms. Nevertheless, optical techniques are limited in providing continuous sensing. Normally, the optical elements, mainly the detector and light source, are placed off the rotating disc and are stationary with respect to it. Therefore, the measurements can only be taken once per

revolution or the disc has to be stopped during measurements[9]. The spin-stop solution is commonly required, and it can lead to undesired delays for time-sensitive experiments or even alter results due to a deceleration in the reaction taking place[27].

Electrochemical sensing on the CD has the potential of providing continuous and real-time sensing thanks to the fact that the miniaturized sensor can be integrated into the disc and rotate with it. Aside from avoiding the previously mentioned undesirable consequences of the spin-stop solution, taking measurements while the CD is spinning provides additional benefits when using electrochemical detection. An electrochemical signal can be enhanced through improved mass transport by convective transfer. With the disc spinning and fluid being pumped, flow of the sample over the electrodes can be achieved leading to a decrease in the Nerst´s diffusion layer thickness. Increasing flow and thus convection hence leads to higher current readouts and therefore lowers LOD and increases sensitivity[28].

The effect of flow on the current signals in 3- and 4-electrode setups was described previously [16,17,18,19]. While the analytical current in a single mode setup benefits from flow enhanced mass transport, leading to a 7-fold increase under flow (500nL/s) compared to the no flow condition as demonstrated in the study conducted by Kamath[29], dual mode currents show little enhancement under increasing flow[30]. This phenomenon is explained by the shearing off of the redox-species concentration profile through flow, and therefore hindering of the redox-species diffusing against the direction of the flow to reach the other working electrode. Kamath et al describe a drop in RA from 37 to 4 on carbon IDAs under flow (500nL/s) when compared to no flow. Higher aspect ratio electrodes suffered less

from the decrease in RA during flow which is explained by the lesser effect of the flow onto the redox-path of analyte between the digits of the electrodes rather than above them[11].

Interfacing electrochemical sensors on the spinning CD with the peripheral equipment has been realized before through utilization of an electrical component transferring the electrical signal to/from the stationary readout unit to the rotating disc. This approach typically entails the use of either stationary carbon brushes sliding across a metal ring that spins with the rotating disc, or a mercury-based rotating electrical connector[9]. The first mechanism, also known as slip-ring, was used by Kim et al. to perform flow-enhanced amperometric detection of C-reactive protein (Fig. 5 (a))[28]. Despite the feasibility of the system, the physical contact between the rings and the brushes induces significant electrical noise while wearing out components and thus changing conductivity and resistance. As far as the second method, Andreasen et al. demonstrated continuous, on-line monitoring of electrochemical experiments with lower amounts of noise[29]. However, this connection method is made up of a rather bulky setup and relies on rather expensive and undesirable mercury as the conducting and connecting substance (Fig. 5 (b)). Rather than establishing electrical contact with the sensors on the disc, recently efforts have been made to develop wireless power and data connections. The first prototypes employing this approach demonstrate that the elimination of physical interface reduces the electrical noise and increases the life-time of the device (Fig. 5 (c))[27].

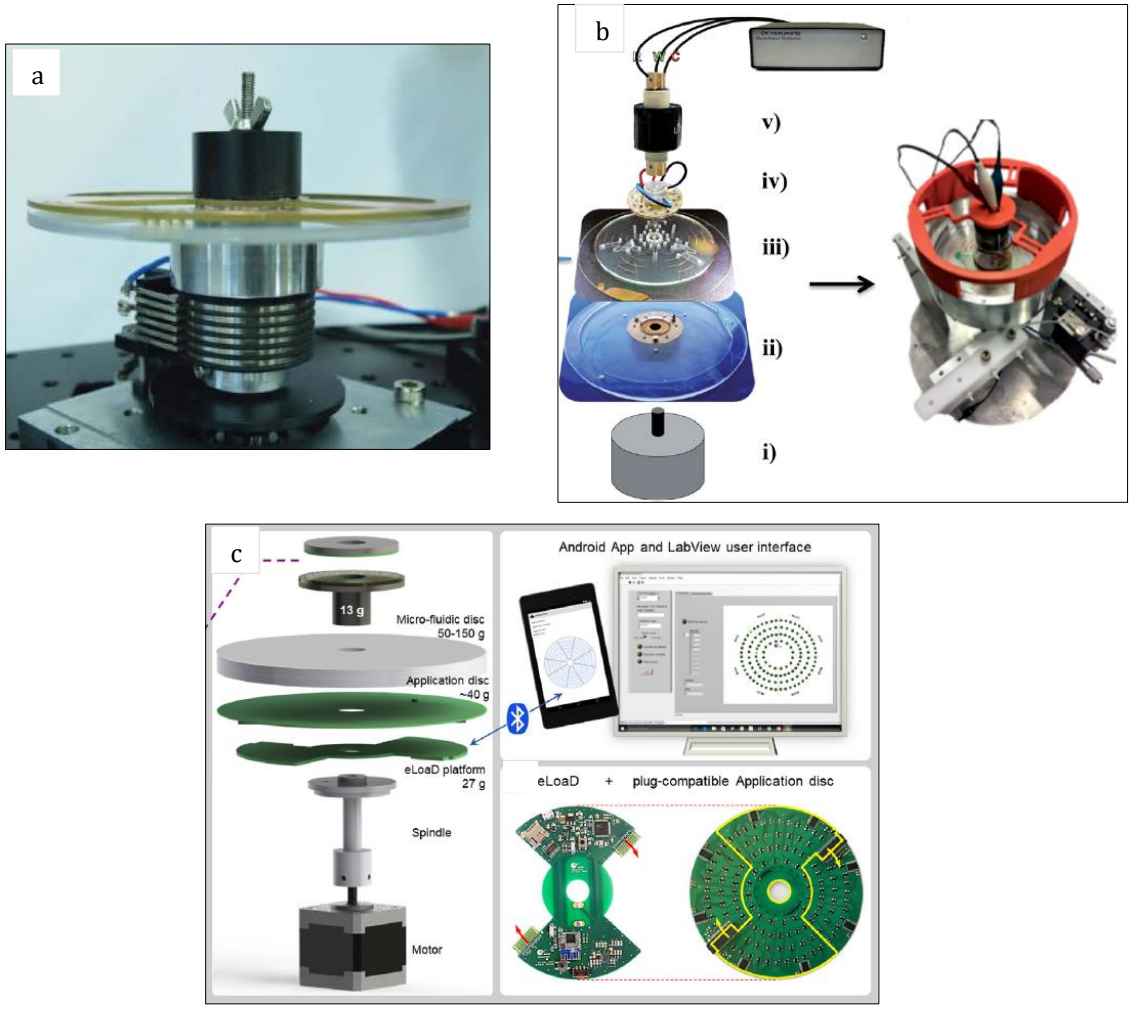

Fig. 5. Current methods to integrate electrochemical detection on a spinning disc. (a) Brush/ring-based slipring approach, with a disc and PCB mounted on the motor shaft[28]. (b) Mercury-based slipring approach, showing all the components of the assembly that include: spinning motor (i), bottom holder (ii), microfluidic disc (iii), custom made plug for interfacing on-disc electrodes with the electrical slipring (iv), and electrical slipring (v)[29]. (c) Wireless powering and data transfer approach, showing all the components of the assembly that include: motor; eLoaD platform consisting of a microcontroller, Bluetooth communication module and SD-card; plug-compatible application disc; and receiver and transmitter coils[27].

Proposed Solution

While most the efforts made in the field of electrochemical detection on a microfluidic CD have relied on the use of microelectrodes in the 3-electrode setup, here we propose the use of the 4-electrode set up in the IDEAs configuration with the goal of achieving an improved sensor performance through redox amplification. Before using the IDEAs for the detection

of the redox analyte resulting from the ELISA assay, we will investigate their hydrodynamic properties including the flow rate dependence of the steady-state current, RA and CE. Besides, the electrochemical behavior of platinum and carbon IDEAs will be compared. It is important to consider, especially for disposable systems, that material choices and manufacturing means for IDEAs vary and severely impact electrode cost.

Regarding the methodology employed to integrate electrochemical detection on the microfluidic CD, we aim to add to the relatively few examples of indirect interfacing approaches by presenting a setup that integrates the analysis instrument, a bipotentiostat (allowing for simultaneous sensing of two working electrodes), to the spinning platform, powering it with a small battery and sending the obtained data via Bluetooth to a stationary desktop computer or mobile phone. Thus, rather than conducting the very low current signals to a stationary instrument, the obtained current signal is sent wirelessly as a binary code and is not affected by transmission errors and noise due to changing electrical contacts.

Despite ample research in all three areas: diagnostics on a CD platform, flow enhanced electrochemical sensing and redox-amplification with IDEAs, to our knowledge, no group has characterized the performance of IDEAs in dual mode under flow conditions on a microfluidic CD nor have such measurements been transmitted wirelessly off the rotating platform.

3. METHODS

The following section describes the approached used to develop a lab-on-a-disc system capable of carrying out an automated ELISA. The system consists of two main components: a central platform that works as a centrifugal and readout unit, and a polymer-based microfluidic disc where the actual assay is carried out. Both components are detailed, along with the complete experimental setup that includes additional hardware and a desktop computer where results are processed and analyzed. Afterwards, the reagents and procedures employed to perform the assay are described. Finally, we present the methods used to analyze the data in order to characterize the sensor performance.

3.1 MICROFLUIDIC DISC DESIGN AND PRINCIPLE OF OPERATION

Two different microfluidic discs were designed in order to accomplish the two major goals of this thesis: one design was used to study the effect of flow on sensor performance, and a second design was used to run the automated immunoassay. Whether the discs need to be reusable is a determining factor in the design. For the first goal, which requires repeated experiments while varying a number of variables such as flow and scan rate, a reusable CD is more convenient. Besides, the high cost of IDEAs is another reason for that. Apart from being reusable, the design has to offer the possibility of removing the IDEAs from the microfluidic disc in order to allow for its cleaning and microscopic observation, which is essential for repeated usage of electrodes. As far as the second design, the disc has to behave as a sample-to-answer system in which cross-contamination needs to be eliminated. Carrying out repeated assays for different samples on the same CD would clearly pose contamination risks, and therefore a disposable CD is needed.

Reusable CD for the Study of IDEAs Hydrodynamic Properties

The reusable CD is a 12-cm-diameter disc with a fluidic layout that includes three identical fluidic units, each one consisting of a fill chamber and a waste chamber connected by a channel and a sensing area in which the IDEAs are exposed to the solution that flows through the channel (Fig. 6 (a). The width of this channel is 1mm and its depth is 100μm. In the sensing area, the channel is perpendicular to the interdigitated array. The predominantly circumferential direction and final serpentine of the channel is used to slow down the flow of solution through the channel, allowing for longer measurement times. As far as the electrodes, both platinum and carbon IDEAs were used (Fig. 6 (b)(c)). Platinum IDEAs consist of 2 working electrodes, counter and reference, with a passivation layer that exposes only a big area of the counter, a small area of the reference, and the interdigitated part of the working electrodes. In this interdigitated array, digits have widths and gaps of 3μm. Electrode height is 90nm. Regarding the carbon IDEAs, their dimensions are identical to those of the platinum IDEAs but with a height of 200nm and 70 digits per working electrode compared to the 65 pairs of the platinum IDEAs. A drop of Ag/AgCl was used on top of both platinum and carbon electrodes as pseudo reference electrodes.

The CD is operated simply by spinning it at a constant speed, which pumps the fluid from the fill chamber to the waste chamber, flowing over the electrode on its way. Valving is not required.

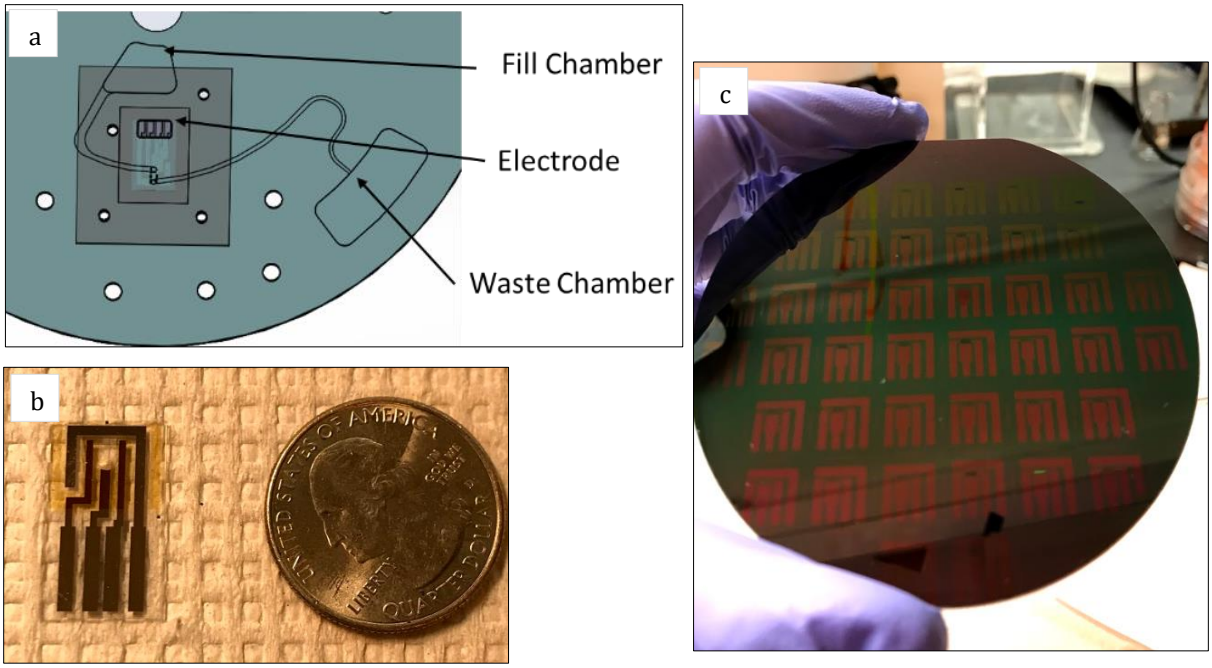

Fig. 6. (a) Fluidic layout of the reusable CD and positioning of either platinum (b) or carbon (c) IDEAs underneath the disc. Carbon IDEAs are shown in the wafer after pyrolysis and prior to cutting.

Disposable CD for Immunoassay

The disposable disc is a 12-cm-diameter disc with a fluidic layout that allows for 3 ELISA assays to be performed in parallel. Each fluidic unit consists of the following chambers: two washing buffer storage chambers, a chamber containing the detection antibody labeled with a redox enzyme, a substrate solution chamber, a reaction chamber containing the capture antibody or antigen, and two waste chambers. These chambers are connected as shown in Fig. 7 (a) by channels with a 1mm width and 0.5mm depth. Channels exiting from the reaction chamber and leading to the waste chambers include serpentines in order to slow down flow of solution, with the goal of providing more effective washing (in the case of the right channel) and more time to perform measurements (in the case of the left channel). Control of flow of solutions from one chamber to the other is achieved using optofluidic valves, which adopt a 2mm-diameter circular shape. The solution resulting from

the ELISA assay is brought to the sensing area by the left channel exiting from the reaction chamber. This channel adopts a bean-shape that allows complete exposure of the electrode to the solution flowing through the channel. A screen-printed circular carbon electrode is used as the electrochemical sensor (Fig. 7 (b)). This electrode has only one working electrode and does not feature an interdigitated array, thus it does not allow for redox amplification. However, due to its low cost and easy accessibility compared to platinum and carbon IDEAs, it is more suitable to be used in the disposable disc.

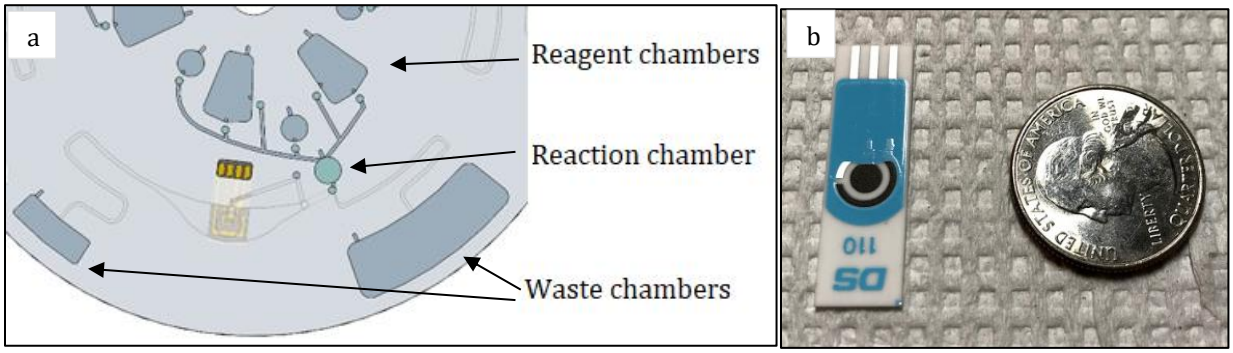

Fig. 7. (a) Fluidic layout of the disposable CD. (b) Screen-printed circular carbon electrode.

The CD is spun at different speeds, oscillated and stopped following a protocol that will be described later in this section. Moreover, in order to sequentially dispense the content of the first four chambers to the central reaction chamber, optofluidic valves are actuated using al low power laser. After each assay step, the content of the reaction chamber escapes the chamber through the capillary valve that leads to the right channel and waste chamber. After the last assay step, the content of the reaction chamber escapes through the optofluidic valve that leads to the left channel and thus, to the sensing area.

3.2 MICROFLUIDIC DISC FABRICATION AND ASSEMBLY

After designing the previously described microfluidic discs using Solidworks 2017 computer aided design software (Solidworks, USA), discs were fabricated by a layered assembly of polymethylacrylate (PMMA) plastic parts and pressure sensitive double-sided adhesives DFM 200 (FLEXcon, USA). For the first design, a modular structure based on an additional holder plate was needed to allow for removal of electrodes.

Reusable CD for the Study of IDEAs Hydrodynamic Properties

The disc assembly consists (top to bottom) of a top adhesive layer sealing the chambers in an underlying PMMA disc, followed by another adhesive layer with microfluidic channels and another PMMA layer with through holes to provide flow to the electrodes. Between the latter PMMA layer and the electrodes, a PDMS layer was placed with a channel perpendicular to the direction of the electrode digits and connecting the through holes while also exposing reference and counter electrodes. Finally, each electrode is held by a PMMA holder which is screwed to the microfluidic disc (Fig. 8). With this, electrodes end up being embedded within a 500µm high microfluidic channel, corresponding to the thickness of the PDMS layer. The total thickness of the whole disc is 8.64mm.

Channels and holes for sample injection and air vent were patterned in the adhesives using the computer-controlled Cameo 3 blade cutter (Silhouette Inc., USA). Chambers and through holes were cut into the PMMA plates using a computer-controlled laser cutter with a 120 W CO2 laser (Trotec Laser Inc., Austria). As far as the IDEAs, platinum IDEAs were

purchased from CH Instruments Inc., and carbon IDEAs were obtained through photolithography of SU8 and subsequent pyrolysis as described elsewhere[11].

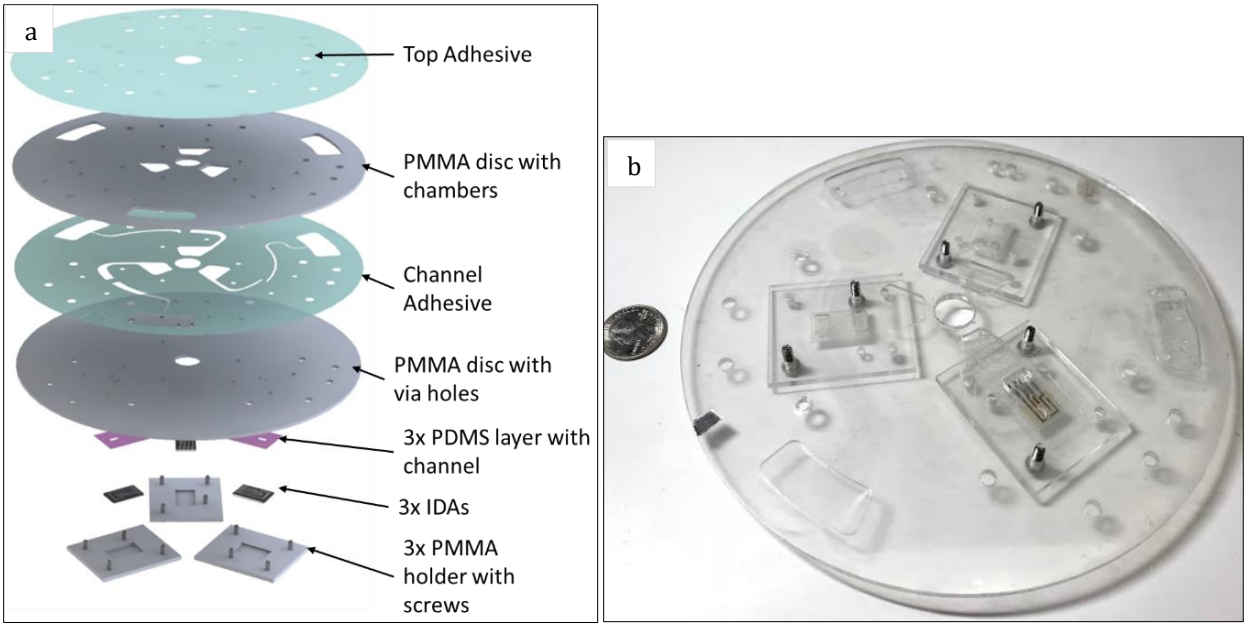

Fig. 8. Components and assembly of the reusable disc. (a) Exploded view showing the different layers of the disc. (b) The assembled disc with platinum IDEAs.

Disposable CD for Immunoassay

The disc assembly is composed of a top and bottom PMMA plates which are bonded using a dark double-sided adhesive. A clear adhesive layer is used on top and bottom of this system in order to seal fluidic compartments (Fig. 9). Holes for sample and reagents injection and air vents are patterned in the top adhesive. As far as the PMMA plates, the top one contains chambers and channels that are cut and etched using the laser cutter. Also using the laser cutter, channels and a recess where the electrode is placed are etched on the bottom PMMA plate. The screen-printed circular carbon electrodes were purchased from DropSense (Spain). The total thickness of the whole disc is 6.65mm.

The top and bottom plates are aligned and bonded using the dark adhesive such that: the electrode is embedded within a 100um high microfluidic channel that is etched in the bottom side of the top plate; and channels at the top and bottom plates overlap at those certain positions where valving wants to be achieved. By applying the approach developed by Garcia-Cordero[15], the middle adhesive blocks the connection between these overlapping channels. Only when the area of the middle adhesive that blocks the connection is melted by heating it up using a laser, the fluidic pathway can be opened, and fluid is allowed to go from the top plate to the bottom plate or vice versa (Fig. 10). While the approach in Garcia Cordero et al. required black dots to be printed by laser printer lithography in the adhesive, here this is not needed since we use a dark adhesive that will directly absorb light at the point where the laser beam is directed. Aside from its critical function in valving, the middle adhesive is also used to isolate the electrode and expose to the solution only its sensing area.

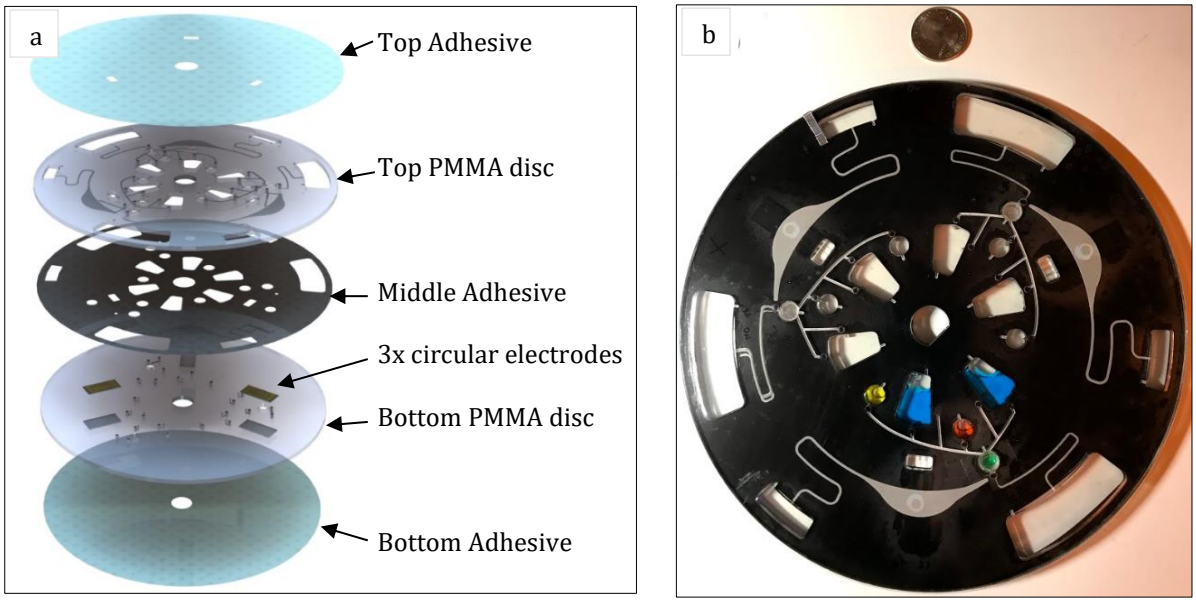

Fig. 9. Components and assembly of the disposable disc. (a) Exploded view showing the different layers of the disc. (b) The assembled disc with platinum screen-printed circular carbon electrodes.

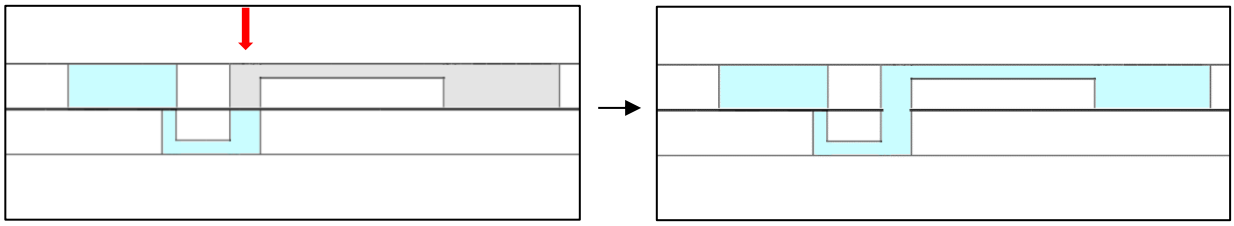

Fig. 10. Optofluidic valve principle of operation. Fluid (in blue) is allowed to go from the first to the second chamber by piercing the middle adhesive at the point where the channels in the upper and lower PMMA parts overlap.

3.3 EXPERIMENTAL SETUP

The experimental setup consists of a central platform that spins the disc and performs electrochemical readout. In order to perform rotary actuation, a spinstand with motor (PMB21B-00114-00, Pacific Scientific Co., USA) and controller (PC3403Ad-001-E, Pacific Scientific Co.) is used. The motor unit allows for autonomous, stand-alone operation by pre-programming rotating speeds in the controller, which is needed to achieve sample handling.

Integration of electrochemical readout in this spinstand is achieved by using a portable, battery powered bipotentiostat (µStat400), which was purchased from DropSense. A holder specially designed to accommodate this instrument was machined and mounted on the motor shaft using a chuck. The bipotentiostat is placed into the holder, and the microfluidic CD is placed on top of it and screwed to the holder (Fig. 11 (a)). In order to stablish electrical connection between the bipotentiostat and the electrode on the CD, a custom connector was fabricated. The original DropSense cable was soldered to this connector, which consists of a PMMA base with copper foil paths and spring-loaded gold pins for contacting the electrode bonding pads. Sensed data is sent by the bipotentiostat to a stationary desktop computer via Bluetooth for further analysis. This computer is also

used to control the bipotentiostat, using the DropView software. The performance of this wireless electrochemical detection setup was compared to the most conventional wired setup that is based on the use of a slip ring. This setup consists in a rotating device including 6 metal rings that is mounted onto the motor shaft and a stationary component with metal brushes that slide across the rings. The latter component is connected to the μStat400 bipotentiostat, which in this case lies stationary. A custom PMMA part with copper traces and spring-loaded pins is used to stablish connection between the electrodes on the CD and the metal rings (Fig. 11 (b)).

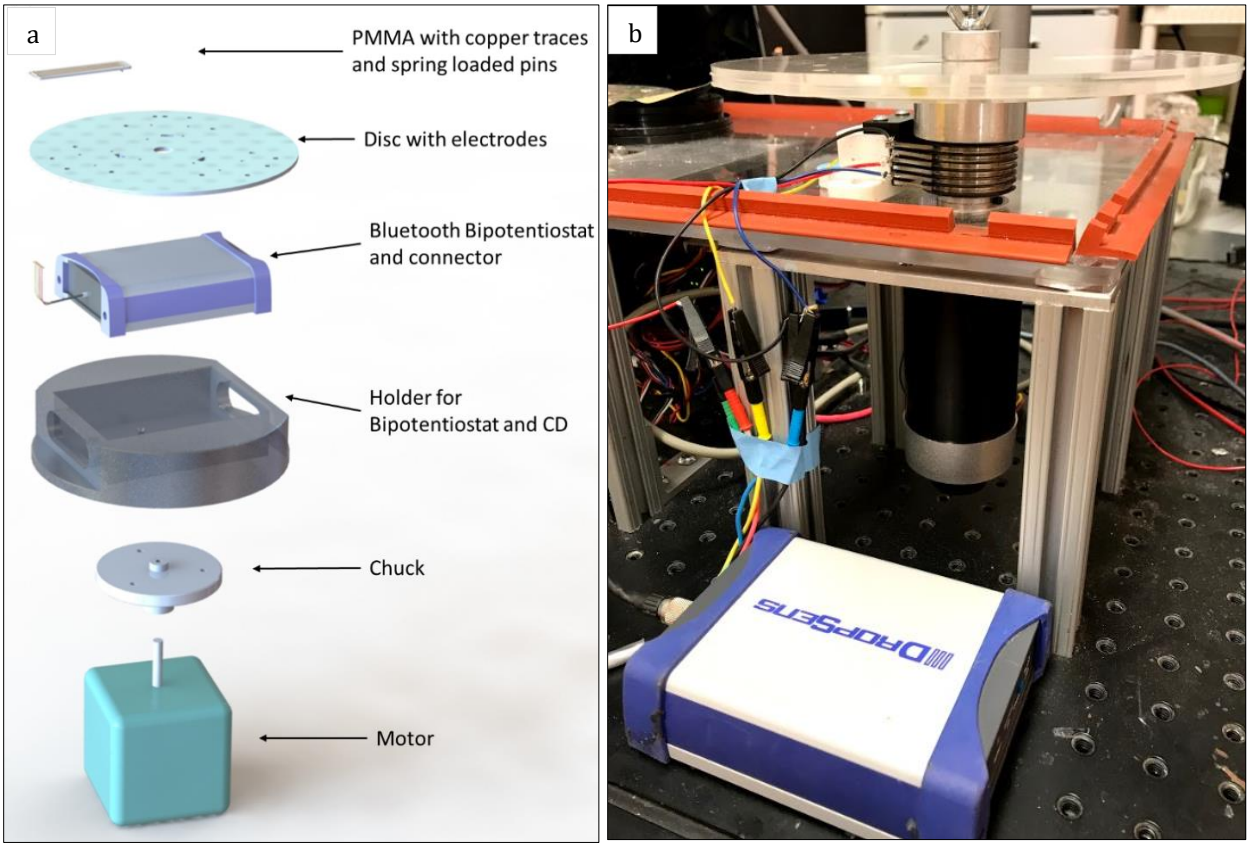

Fig. 11. Central platform to spin the disc and perform electrochemical readout. (a) Exploded view of the wireless setup. (b) Image of the wired setup.

Additional hardware is needed to perform the experiments (Fig. 12). A stroboscopic optical setup is used for the general control of fluidics and analysis of flow rates. This includes a trigger (D10DPFPQ, Banner Engineering Corp., USA) that is installed to trigger a high-speed camera (Area Scan A311fc, Basler AG, Germany) and a stroboscope (DT-311A, Nidec-Shimpo Corp., USA) at each single rotation of the disc. This allows visualization of the fluidics on the desktop computer while the disc is spinning. Regarding the immunoassay experiments, two additional components are needed: a low power laser diode (100-500 mW) and an infrared (IR) lamp. The laser is used to actuate the optofluidic valves, and the IR lamp is used to perform the incubation step that is part of the immunoassay. These components are placed over the disc at a distance providing optimal laser focusing and heating. Steel bars and custom holders are used to hold these devices, allowing for easy repositioning. Both devices are powered using independent, portable DC sources and are operated manually.

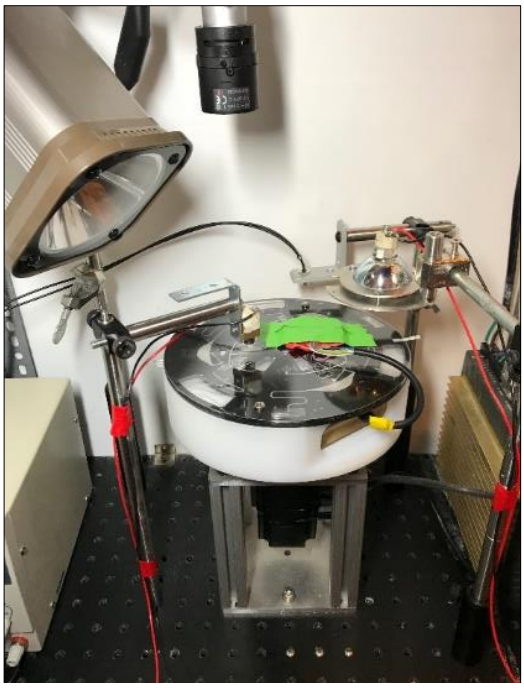

Fig. 12. Complete experimental setup.

3.4 REAGENTS

Performance of IDEAs under static and flow conditions was characterized using ferricyanide-ferrocyanide redox-couple. Solutions were prepared with 1mM, 3mM, 5mM, 7mM and 9mM of both ferricyanide and ferrocyanide and a supporting electrolyte of 2M KCl. One solution was prepared as blank (i.e. only containing 2M KCl) for measuring noise from the setup.

Automated immunoassay on the CD was demonstrated using a commercial ELISA kit for qualitative determination of antibodies against Plasmodium in human serum or plasma (IBL International, Germany). This kit includes a number of reagents, controls and wells coated with recombinant Plasmodium antigens that were used on the CD to electrochemically detect malaria. Each of the following reagents were introduced in their corresponding chambers: 600µl of diluted washing buffer in each washing buffer storage chamber; 100ul of peroxidase labelled antibodies to human IgG/IgM in phosphate buffer, used as the detection antibodies; and 100ul of TMB 3,3',5,5'-tetramethylbenzidine (TMB), used as the substrate solution. As per the component that has to capture the antibodies against Plasmodium, one of the wells coated with recombinant Plasmodium antigens was custom cut and fitted into the reaction chamber. Finally, 100ul of the diluted human serum or plasma sample that wants to be analyzed is injected to the reaction chamber. After that, the disc is ready to be mounted on the spin stand and the automated assay can begin. In this work, real samples were not available. Thus, positive, negative and cutoff malaria controls included in the ELISA kit were used to demonstrate the immunoassay on the CD.

3.5 PROCEDURES

Study of Signal Quality in Wired and Wireless Setups

Performance of the conventional slip ring setup and of the novel wireless interfacing approach developed in this work were compared by carrying out cyclic voltammetry measurements on the disc. The disc used in these experiments was the same that was used for the study of IDEAs hydrodynamic properties, yet in this case the CD contained the screen-printed circular carbon electrodes instead of IDEAs. Ferricyanide-ferrocyanide

solutions were used as the redox analyte, and the voltage was scanned form -0.4V to 0.4V at 2V/s and 0.1V/s. Measurements were taken while the disc was both stopped and spinning at different RPMs. Resulting signal quality was compared in terms of noise.

Study of IDEAs Hydrodynamic Properties

First, we characterized the performance of platinum and carbon IDEAs on the disc in terms of redox amplification and sensitivity. This involved repeated experiments consisting in: loading 300µl of the ferricyanide-ferrocyanide solution into the fill chamber of the disc; spinning the disc at 200 RPMs; stopping the disc after verifying that the channel over the electrode was filled with solution; and finally carrying out cyclic voltammetry in both single and dual modes.

After performing the stationary measurements, the effect of flow on platinum IDEAs was investigated. After loading 300µl of the ferricyanide-ferrocyanide solution, the disc was mounted on the centrifugal platform and spun while carrying out cyclic voltammetry in both single and dual mode. This procedure was repeated for different spin speeds: 0, 100, 200, 300 and 400RPMs. The flow rate generated by these spin speeds was quantified through visualization of the fluidics using the stroboscopic optical setup, which allowed to determine the time that it took for the 300µl of solution to go from the fill to the waste chamber. Further details about electrochemical measurement settings and cleaning procedures are described below.

Platinum IDEAs:

For single mode operation, the potential was scanned from 0V to 0.6V in 0.002V steps at a scan rate of 0.02V/s. Dual mode was conducted using the same step size and scan rate with one working electrode scanned from 0.1V to 0.6V and the second working electrode kept constant at 0V. This scan rate leads to peak currents in no-flow and low RPM conditions due to the diffusion-limited mass transfer, while allowing for reaction limited currents at higher flow rates. Choosing a lower scan rate was not feasible as it did not allow for the completion of forward and backward scan with a maximum fill volume of 300μL.

Platinum electrodes were cleaned, once degradation in performance was observed. Cleaning of the Pt electrodes consisted of depositing a drop of 0.1N sulfuric acid solution on the sensing area of the Pt electrodes and conducting 20 cycles of cyclic voltammetry (CV) with sweep range from 0V to 1.5V at a scan rate of 0.1V/s. This procedure was followed by rinsing the IDEA with distilled water and drying with filtered nitrogen. When subsequent control under microscope showed debris between the digits of the IDEA, the interdigitated electrodes were carefully polished parallel to the digit direction with a gloved finger under flowing distilled water. Drying and control with a microscope was repeated until all the debris was removed.

Carbon IDEAs:

Similar to platinum electrodes, carbon electrodes were utilized in single as well as dual mode. For single mode the best scan range was 0V to 0.5V. The scan rate in single as well as dual mode was 0.01V/s. Due to the lower conductivity of carbon as compared to platinum,

the iR drop of carbon electrodes was higher. As the portable bipotentiostat did not allow for iR compensation, larger scan ranges were necessary to take full advantage of redox-amplification when working with carbon electrodes. The dual mode curves for carbon electrodes were observed to approach a plateau around 1V when scanning at 0.01V/s. However, such large scan ranges lead to the disintegration of the counter electrode and therefore to the reduction of the lifetime of the carbon electrode. To allow for the maximum sweep range and avoid early disintegration of the counter electrodes, the pH level of the solutions was measured and adjusted to a pH of 8 using sodium hydroxide. Nevertheless, to allow for an increased lifespan of the electrodes, sweep ranges in dual mode were limited to 0.1V to 0.6V for experiments on the CD. Due to the lower cost (about $5 per carbon electrode versus about $200 for a platinum electrode), carbon electrodes were replaced once signals started diverging rather than cleaned and used again.

Immunoassay on Well Plate

Commercial ELISA tests were first carried out off the CD following the manufacturer's instructions. However, the TMB product that results from the assay was analyzed electrochemically rather than optically. These experiments were aimed at characterizing the cyclic voltammetry and chronoamperometry curves of TMB, and at demonstrating that TMB can work as a substrate to electrochemically detect the presence of antibodies against Plasmodium.

Following the manufacturer's protocol, 100µl of each control were dispensed into the wells coated with recombinant Plasmodium antigens (P. falciparum, P. vivax) of the microplate included in the kit, and incubated for 1 hour at 37°C. Afterwards, the content of the wells

was removed, and three consecutive washing steps were performed, each one with 300µl of diluted washing buffer (1:10 in distilled water). 100µl of HRP-conjugated antibodies were dispensed into each well and incubated for 30 minutes at room temperature (20-25°C). The content of the wells was removed and 3 washing steps were repeated afterwards. Finally, 100µl of TMB substrate solution were dispensed into the wells and incubated for 15 minutes at room temperature in the dark. The whole procedure was performed doing manual pipetting. A scheme of the assay and is found in Fig. 13.

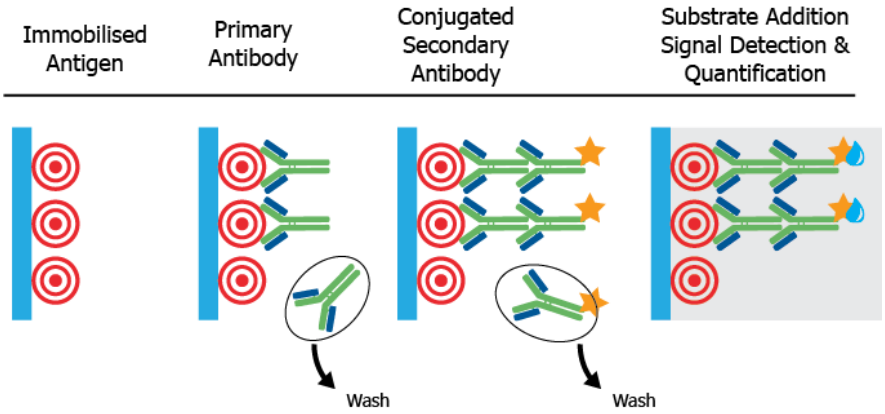

Fig. 13. Scheme of the assay. Note: primary antibody is the antibody against Plasmodium that is present in the sample and wants to be detected.

After the 15-minute incubation, 100µl of sulfuric acid were dispensed to some of the wells. This chemical acts as stop solution, i.e. it stops the enzymatic activity of HRP, providing a stabilized TMB product that can be analyzed optically using a spectrophotometer or in our case, electrochemically. As far as those wells in which no stop solution was applied, electrochemical measurement had to be performed immediately after the 15-minute incubation. In order to perform the measurements, screen printed circular carbon electrodes (such those integrated in the disposable disc) were used. 50µl of the TMB product were dispensed on the electrodes, which were connected to the DropSense

bipotentiostat using a connector from the same company. Cyclic voltammetry and chronoamperometry were performed by controlling the bipotentiostat with the DropView software. For cyclic voltammetry, the working electrode potential was swap from -0.2V to 0.6V at a scan rate of 50mV/s. For chronoamperometry, a -0.2V potential was applied.

Immunoassay on-CD

The commercial ELISA is automated using the disposable CD and centrifugal platform, following the same steps and incubation times established by the manufacturer. The on-CD protocol can be simplified as the repetition of the following process: the reagent is dispensed into the reaction chamber and incubated for the required amount of time, the reagent is then flushed out to the waste chamber, and finally washing buffer is dispensed to and afterwards removed from the reaction chamber.

With the disc with all the preloaded reagents (washing buffer, TMB substrate solution, and the HRP-conjugated antibodies), 100µl of the sample or control are injected into the reaction chamber and the disc is mounted on the spin stand. Then, the motor starts rotating following the spin program detailed in Table 1. Every time that an optofluidic valve needs to be operated, the disc is brought to a halt, the peripheral mobile laser is aligned over the valve, and the valve is irradiated for 10 seconds. As far as the protocol described in Table 1, sample incubation is performed during 1 hour with the IR lamp on. During this hour, 5-minute intervals of oscillation and halt are alternated. Oscillation intervals, in which the disc repeats cycles of acceleration and deceleration (±1 Hz/s), are used to promote efficient binding between antibodies in the solution and the antigens immobilized in the bottom of the well. After the incubation, the residual solution is removed into the

waste chamber by spinning the disc at the high speed (800 RPMs) which allows the capillary valve to burst. Next, two washing steps are applied by actuating valves #1 and #2. Each washing step consists in: actuating the respective valve, spinning the disc at the low speed (300 RPMs) to transfer 300µl of washing buffer into the reaction chamber, oscillate the disc for 20 seconds to improve washing, and finally remove the washing buffer into the waste chamber by spinning the disc at the high speed. Thanks to the fluidic layout, these two washing steps can be performed having only one washing buffer storage chamber. Afterwards, valve #3 is actuated and the conjugate is transferred into the reaction chamber and incubated for 30 minutes with the same 5-minute intervals of oscillation. The residual solution is flushed out to the waste chamber, and two washing steps are applied by actuating valves #4 and #5 and following the same washing procedure as before. Finally, the TMB solution is transferred to the reaction chamber after actuating valve #6 and incubated for 15 minutes while oscillating the disc. Afterwards, valve #7 is opened and the disc is spun at 300RPMs. This low spin speed is not high enough to prime the capillary valve, thus preventing the TMB to go to the waste chamber and allowing it to enter the left channel that brings it to the electrodes. After verifying that the three electrodes (working, counter and reference) are completely covered by solution, electrochemical measurements can be performed. Measurements were taken during 35 seconds with the CD spinning at 300 RPMs, allowing for flow-enhanced signals. Chronoamperometry was performed with a -0.2V potential applied to the working electrode.

Table 1. Spin speed program to perform the automated ELISA on the disc.

Spin No.	Speed (RPM)	Time (s)	Operation
1	Oscillation	3600	Sample incubation with mixing
2	800	15	Remove residual solution
3	300	5	Open valve #1 to transfer 1st washing buffer
4	Oscillation	20	Mix washing buffer and residue in reaction chamber
5	800	15	Remove 1st washing buffer
6	300	5	Open valve #2 to transfer 2nd washing buffer
7	Oscillation	20	Mix washing buffer and residue in reaction chamber
8	800	15	Remove 2nd washing buffer
9	300	5	Open valve #3 to transfer conjugate
10	Oscillation	1800	Conjugate incubation with mixing
11	800	15	Remove residual solution
12	300	5	Open valve #4 to transfer 1st washing buffer
13	Oscillation	20	Mix washing buffer and residue in reaction chamber
14	800	15	Remove 1st washing buffer

15	300	5	Open valve #5 to transfer 2nd washing buffer
16	Oscillation	20	Mix washing buffer and residue in reaction chamber
17	800	15	Remove 2nd washing buffer
18	300	5	Open valve #6 to transfer TMB substrate solution
19	Oscillation	900	TMB incubation with mixing
20	300	60	Open valve #7 to transfer TMB to sensing area Flow-enhanced electrochemical measurements while the TMB flows through the final serpentine

3.6 DATA ANALYSIS

Cyclic voltammetry (CV) and chronoamperometry curves were first filtered with Origin 2018b (Originlab Corp., USA) using Fast Fourier Transformation (FFT) filtering in order to remove oscillatory noise from spinning of the disc. Furthermore, a baseline for each CV was stablished using a first order tangent based on 5 points in the linear area of each curve. Afterwards, several variables were analyzed. In CV curves, peak and limiting currents were quantified. In single mode, peak current is the highest current recorded in the forward scan. In both single and dual modes, limiting current is the one reached at the steady-state which is approximated to be the one recorded at the highest potential. Using the limiting current, a calibration curve was established for each spin speed based on measurements of varying concentrations (i.e. 1mM, 3mM, 5mM, 7mM, 9mM at spin speeds of 0RPM, 100RPM,

200RPM, 300RPM, 400RPM respectively). The curves were quasi linear in the range of the tested solutions, and the obtained slope equals the sensitivity at the respective spin speed. Another variable to analyze was the LOD, which was considered to correspond to 3 times the standard deviation of the CV for the blank solution in a range of 0.5V around the potential of the peak currents in solutions with the redox couple present. The standard deviation, which is also used as a measurement of noise, was measured using Origin 2018b. As far as chronoamperometry curves, we took the average of the currents recorded during the last five seconds as an approximation of the limiting current.

In order to assess dual mode performance of IDEAs, RA and CE variables were computed. RA was calculated as the ratio between the limiting current in dual mode and the limiting current in single mode. CE was calculated as the ratio between the limiting current of the collector and the limiting current of the generator.

Regarding the study of the influence of flow on IDEAs performance, three different models were used. Single mode limiting currents were calculated with respect to the flow rate ν according to[11]:

$$\mathbf{i_L = 1.47nFC(DA/B)^{\frac{2}{3}}\nu^{\frac{1}{3}}} \quad (1)$$

where n is the number of electrons transferred, F is Faraday's constant, C is the bulk concentration, D is the diffusion constant, A the area of electrodes and B the height of the channel. Therefore, flow is expected to increase with current as the cubic root until the reaction rate at the electrode surface becomes limiting.

Dual mode limiting currents without flow for different concentrations were calculated according to Aoki et al.[31]:

$$\mathbf{i = mbnFCD\left(0.637\ln\left(\frac{2.55}{x}\right) - 0.19x^2\right)} \quad (2)$$

with m the number of digits per working electrode, b the length of each digit and x the width of the digit divided by the width plus the gap. The diffusion constant of potassium ferri-ferrocyanide was assumed at 7.26E10-6$\mathbf{cm^2/s}$ [32].

As far as dual mode limiting current with flow, RA and CE are expected to decrease with increasing flow rates due to shearing off of species. Dual mode currents with flow at different concentrations were calculated according to the model by Morita et al[30]:

$$\mathbf{i_L = mnFCQ\frac{W_e}{W_c}\nu} \quad (3)$$

with m the number of digits per working electrode, $\mathbf{W_e}$ the electrode width, $\mathbf{W_c}$ the channel width, and Q the coulometric yield which is calculated as:

$$\mathbf{Q = 1.467p^{\frac{2}{3}}, \quad 0 < p \leq 0.01} \quad (4)$$

$$\mathbf{Q = 1 - 0.896e^{-1.559^2 p} - 0.061e^{-4.857^2 p} - 0.018e^{-8.134^2 p}, \quad p > 0.01} \quad (5)$$

where $\mathbf{p = LD\frac{W_C}{d\,\nu}}$ with L the electrode length, and d the channel thickness.

4. RESULTS

The following section presents the results of the work carried out in this thesis towards the achievement of the three major goals listed in the introduction. First, the integration of electrochemical detection on a centrifugal platform through wireless data transfer is characterized and compared to the slip ring setup. Second, results from the study of IDEAs hydrodynamic properties are presented. Finally, use of the developed platform for qualitative detection of antibodies against Plasmodium in human serum or plasma is demonstrated.

4.1 SIGNAL QUALITY IN WIRED AND WIRELRESS SETUPS

Comparative analysis of signal quality in wired and wireless setups was carried out by running cyclic voltammetry measurements in both stationary and rotating conditions. Fig. 14 shows CV curves obtained for a solution containing 2mM of ferricyanide-ferrocyanide and 2M of KCl. High levels of noise appear when introducing rotation to the slip ring measurements, which hinders selection of peak and limiting current values as well as the study of the effect of flow on these values. Unlike the wired setup, the wireless setup provides minimum levels of noise that allow for stable measuring performances while spinning the disc. In this case, the influence of flow on peak and limiting currents can be investigated.

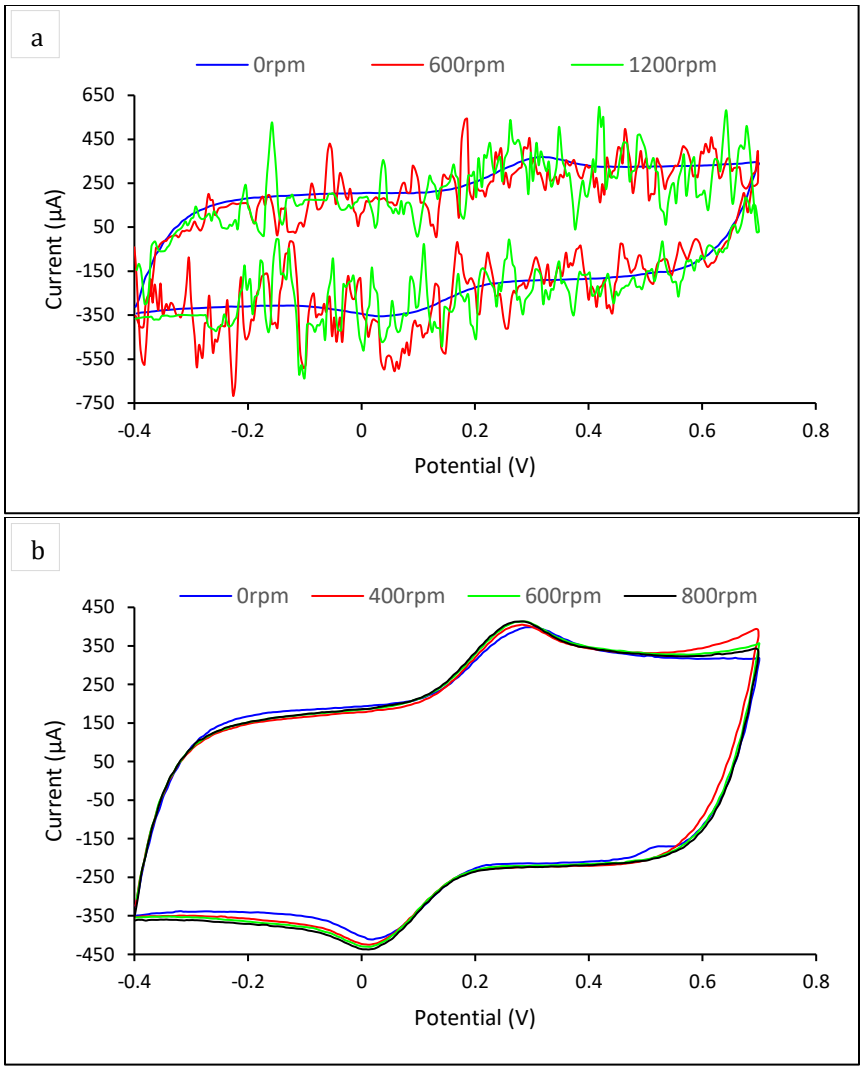

Fig. 14. Cyclic voltammetry curves obtained for a 2mM ferri-ferrocyanide solution using the slipring setup (a) and the wireless setup (b) at different spin speeds. Scan rate = 2V/s.

Low signal quality in the slipring setup is primarily attributed to the poor and unstable electrical connection that exists between the metal rings and the brushes. Repeated use of the setup wears these components out, and leads to the need for periodical replacement. Even though replacement was not an option because new components were not available, we improved the measuring performance of the slipring setup by fabricating a new PCB and by scanning at lower scan rates. Fig. 15 shows CV curves obtained at 100mV/s for the same 2mM solution. A significant decrease in noise level was achieved in comparison to

previous measurements. It could be clearly distinguished that increasing spin speed leads to higher peak and limiting currents, which is explained by the improved mass transport phenomena.

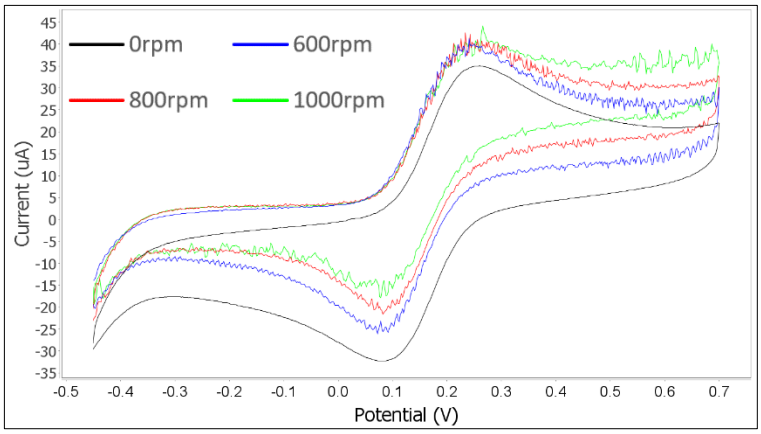

Fig. 15. Cyclic voltammetry curves obtained for a 2mM ferri-ferrocyanide solution using the slipring setup with improved PCB at different spin speeds. Scan rate = 100mV/s.

Despite the previous improvement in the slipring setup, signal quality remains superior when using the wireless setup. In Fig. 16 we show a CV measurement obtained at 2V/s for a blank solution while spinning the disc at 600RPMs. The noise level is reduced from 19.09µA when using the wired setup to 1.84µA when using the wireless setup. In addition to the reduction in noise, the higher stability of measuring performance over time boosts the need for a wireless system.

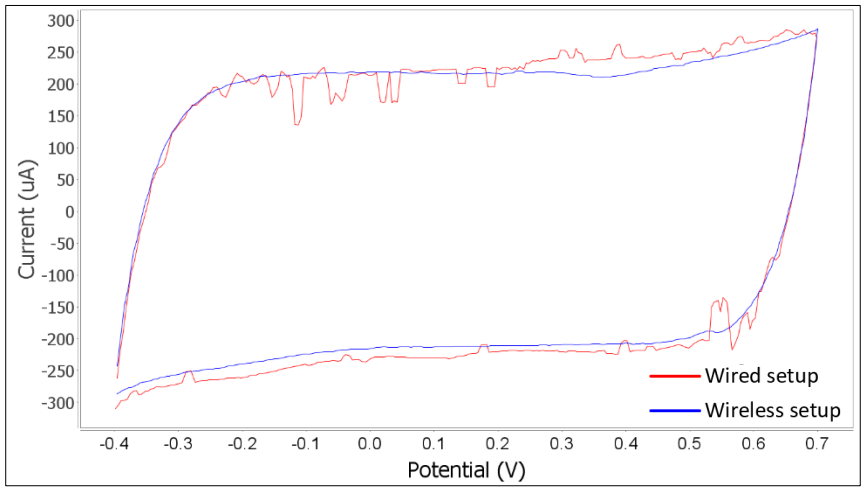

Fig. 16. Cyclic voltammetry curves obtained for a blank solution using the slipring setup and the wireless setup at 600rpm. Scan rate = 2V/s.

4.2 EFFECT OF FLOW ON ELECTROCHEMICAL SENSOR PERFORMANCE

Stationary Electrochemical Sensor Performance

First, stationary sensor performance of both platinum and carbon IDEAs on the disc was established in single and dual mode with a solution of 5mM ferri-ferrocyanide. Potentials were measured versus Ag/AgCl. In Fig. 17 we show the resulting CV curves for platinum (a) and carbon (b) electrodes. Measurements for both electrodes are summarized in Table 2.

Table 2. Stationary measurements in dual and single mode on platinum and carbon IDAs.

	Platinum IDA	Carbon IDA
Single mode peak current	5.2μA	9.9μA
Generator current	37.7μA	165.5μA
Collector current	37.5μA	166.7μA
Redox amplification (with respect to peak current)	7.25	16.7
Collector Efficiency	0.99	1.0

While with platinum IDEAs the area of the working electrodes exposed to fluid is restricted to the interdigitated digits by a passivation layer added by the manufacturer, for carbon IDEAs a small area of the traces between digits and bonding pads may be exposed to the solution as well. Even though the PDMS layer that is placed on top of the electrode is designed to expose only the digits, slight misalignments can make adjacent areas to the digits to be also exposed. This explains the generally higher currents with carbon

electrodes as well as a CE slightly larger than 1 (due to unequal areas of the two working electrodes exposed to solution). Furthermore, it can be seen from Table 2 that carbon IDEAs have a higher RA than platinum IDAs. This can be explained by the higher aspect ratio of the carbon IDAs compared to platinum IDAs. The higher aspect ratio of the carbon electrodes does not only increase the surface area for electron exchange but also decreases the diffusion path in a linear diffusion profile between electrode digits as compared to an elliptical diffusion profile atop of the electrode digits in the more planar Pt case[11]. It might be noted here that with different carbon electrode geometries carbon IDAs amplification factors of up to 38 were obtained. Predicted dual mode current (based on Equation 2) for platinum IDAs in dual mode is in good agreement with experiment, with calculated and experimental value respectively of 45.1μA and 37.7μA. Possible reason for lower than calculated values in the experiments is contamination of the electrode surface[33].

In Fig. 17(c) and 17(d) we show the CVs for platinum IDAs in stationary on disc measurements for various concentrations in single and dual mode respectively. For the dual mode graph, baselines were subtracted from measurements for better visualization of the current increase at higher concentration. Based on the measurements shown in Fig. 17, calibration curves for single and dual mode of platinum electrodes were obtained. These are shown in Fig. 18. The sensitivity was calculated from the slope of calibration curve as 0.39μA/mM and 6.7μA/mM for single and dual mode in stationary measurements respectively. As it can be seen from these values and Fig. 18, the sensitivity for dual mode is higher than for single mode, thus affording a lower LOD of 10.14nM in dual mode versus 63.51nM in single mode at 0RPM (based on average noise level of 21.5pA in measurement).

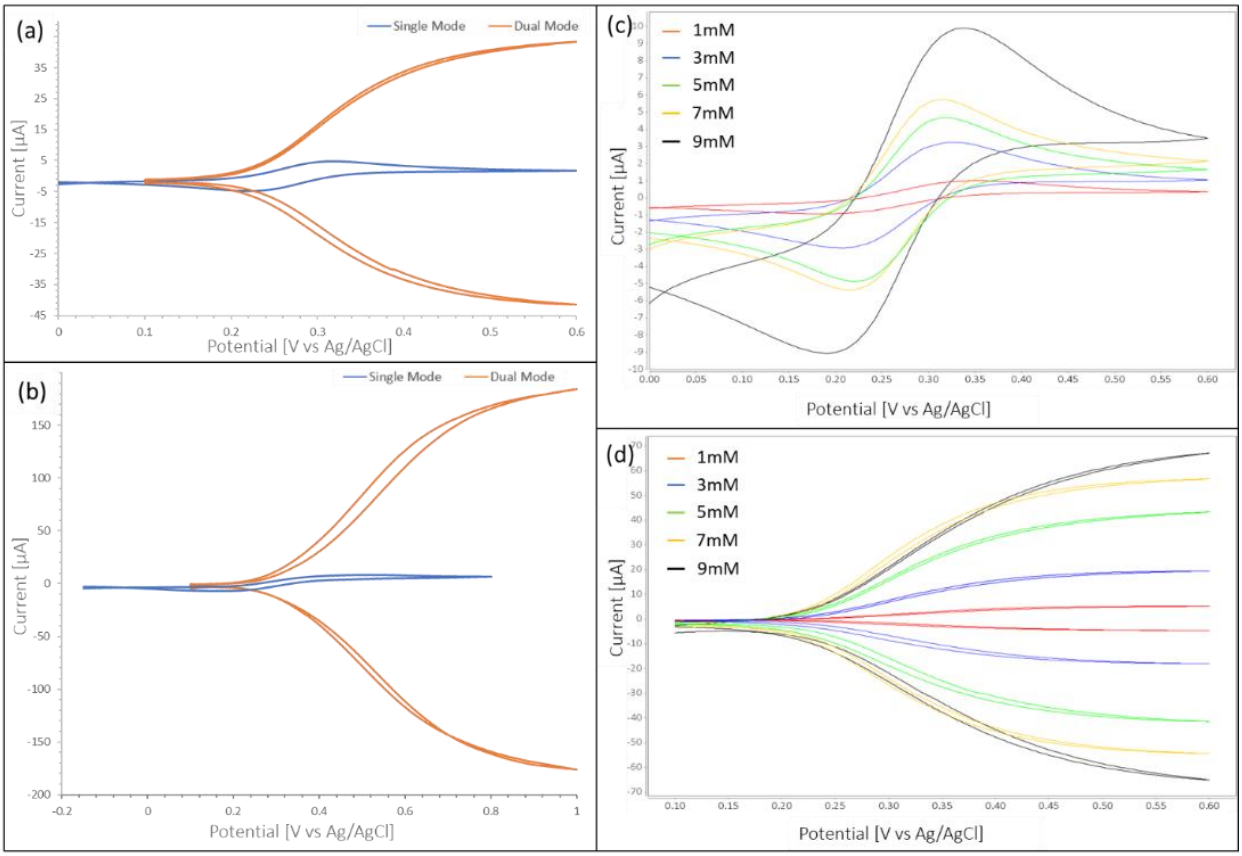

Fig. 17. Single and dual mode CVs for (a) platinum IDEA and (b) carbon IDEA. (c) Single mode CV for platinum IDEA with concentrations 1mM through 9mM ferri-ferrocyanide (d) Dual mode CV for platinum IDEA with concentrations 1mM through 9mM ferri-ferrocyanide. Scan rate = 20mV/s.

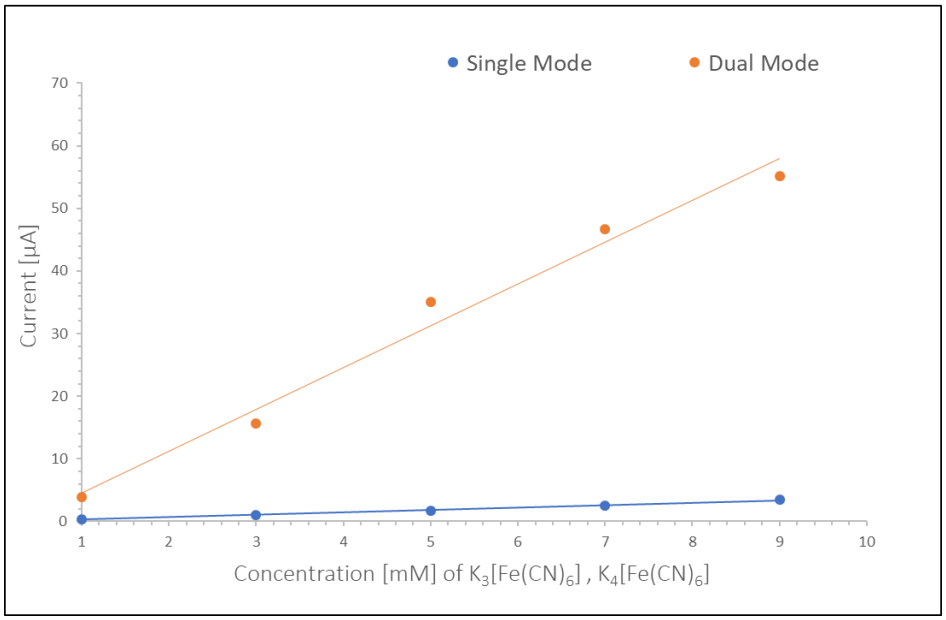

Fig. 18. Calibration curve for single and dual mode, platinum IDEA, stationary measurements.

Effect of Flow Velocity on Redox Cycling

The effect of flow on the measured currents in single and dual mode can be seen in Fig. 19(a) and (b) respectively. The graphs show the CV curves for 7mM ferri-ferrocyanide solution. It is observed from Fig. 19(a) that single mode CV moves from a diffusion limited curve with peak current to a reaction limited curve for increasing flow rate. The dual mode curves Fig. 19(b) show less impact of flow on current but the current still increases with increasing flow.

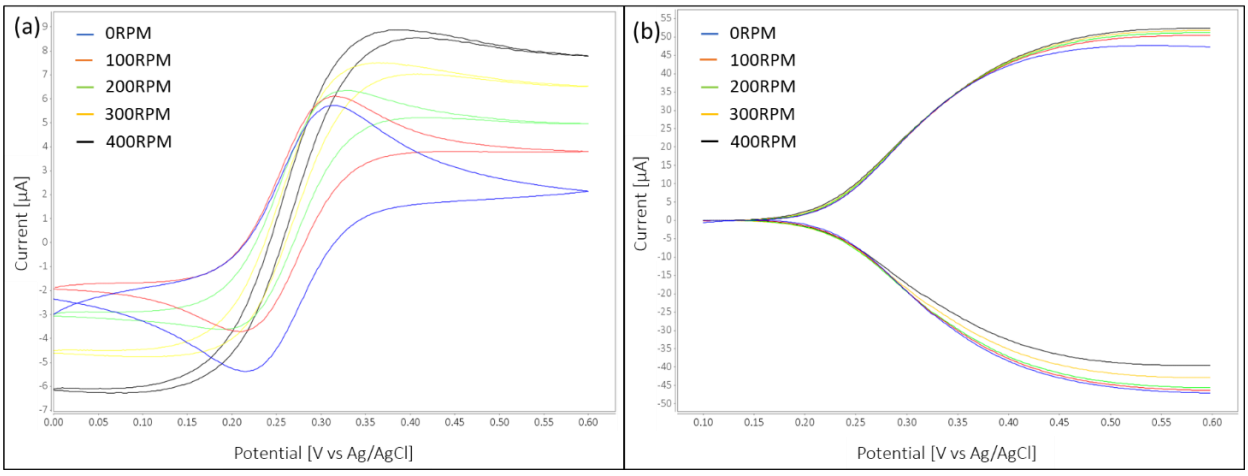

Fig. 19. (a) Single mode platinum IDEA CV for increasing flow rates. (b) Dual mode CV for platinum IDEA for different flow rates. The baseline was subtracted from curves in dual mode for better visibility of the current increase with increasing flow rate. Scan rate = 20mV/s.

Effect of flow on single mode limiting current is also explained analytically by applying Equation 1. To allow for the calculation of single mode currents for different spin speeds, the flow rate at different spin frequencies was measured and results are shown in Fig. 20(a). Calculation (based on Equation 1) and experimental single mode limiting currents were in good agreement (Fig. 20(b)) and linear with ν^(1/3), demonstrating that flow over the electrodes generated by the spinning disc effectively increases mass transport resulting in an increase in the current.

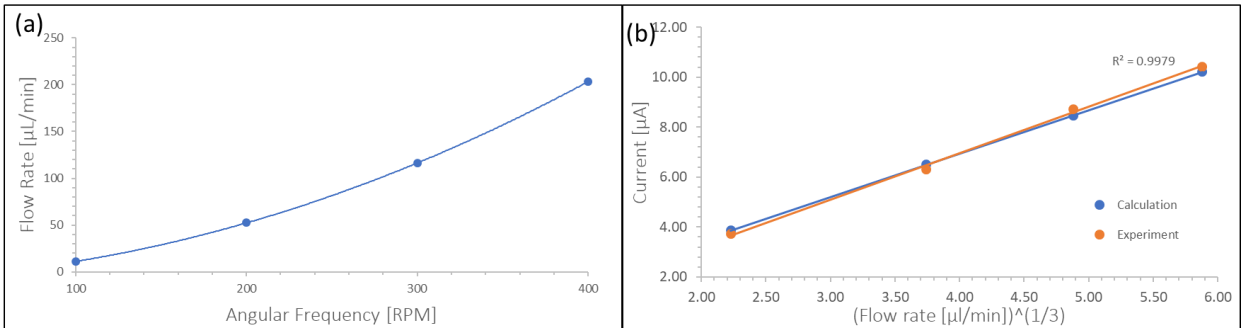

Fig. 20. (a) Relation between angular frequency and flow rate. (b) Calculated (blue) and experimental (red) single mode limiting currents for increasing flow rate, using a platinum IDEA and a solution of 7mM ferri-ferrocyanide.

As far as the effect of flow on dual mode limiting currents, experimental results were compared to theoretical values defined by Morita's model[30]. Using the flow rates previously obtained, Equation 3 was applied. Table 3 shows a comparison of experimental and predicted dual mode currents for a 1mM ferri-ferrocyanide solution at increasing flow rate. Overall experimentally obtained currents are by a factor of 4.19 to 9.83 higher than predicted currents, which could be due to smaller than assumed channel geometry (height and width of channel depends on compression and thus deformation of PDMS layer) as well as due to neglecting of species trapped between the digits at the height of the electrodes, which are less affected by flow.

Table 3. Comparison of predicted and measured currents in dual mode for a 1mM ferri-ferrocyanide solution at spin speeds of 100, 200, 300 and 400RPMs.

	100 RPM	200 RPM	300 RPM	400 RPM
Predicted Current [uA]	0.481	0.852	1.112	1.340
Measurement [uA]	4.727	4.922	5.108	5.621

Further characterization of influence of flow on dual mode involves assessment of RA and CE variables. In Fig. 21(a) we show the decrease of RA with respect to the limiting current from 16.2 to 4.6 and Fig. 21(b) shows the decrease in CE from 0.94 to 0.67 both with increasing flow rate. The RA and CE values are based on average measurements of all concentrations at the respective flow rates. This behavior is as expected as the increasing flow shears off redox species and precludes it from repeated redox cycling.

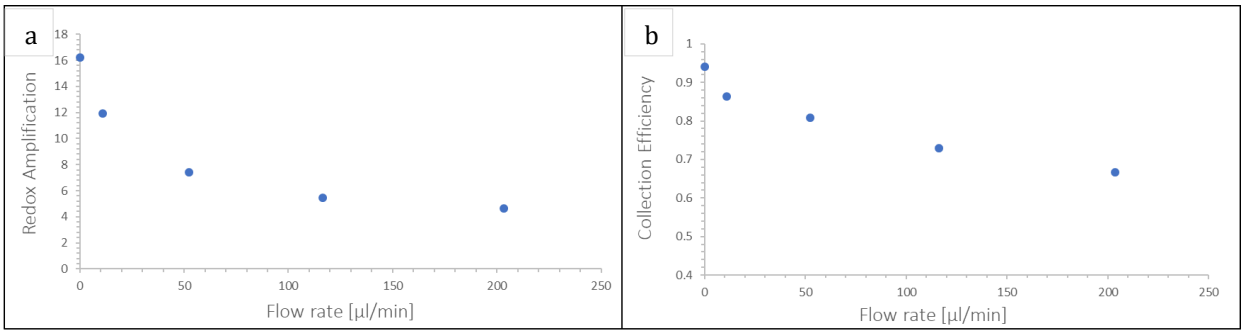

Fig. 21. (a) Average RA versus flow rate. (b) Average CE versus flow rate.

Flow-Enhanced Electrochemical Sensor Performance

Despite a decreasing RA, the dual mode with flow affords the highest sensitivity of 6.99µA/mM and, in conjunction with average constant noise level (after FFT filtering of oscillatory noise from the rotation) of 21.5pA, leads to the lowest LOD of 9.23nM. Therefore, based on this study, dual mode CV with flow should be used for best electrochemical measurement performance at low concentrations (see Table 4). It is important to notice that the beneficial effect of flow on sensor performance has been demonstrated here for slow flow rates. At the slow flow rates considered in this study, increased currents can be achieved by the following phenomena happening at the same time: improved mass transport through flow, and redox cycling. However, sensor

performance at high flow rates could eventually worsen due to the complete mitigation of redox cycling by flow.

As far as the scan rate employed, in this study we consider slow scan rates (20 mV/s) that allow redox species to cycle a greater number of times, since the time available for redox cycling is longer. This makes dual mode currents to be always greater than single mode currents. Nevertheless, in CV measurements with very high scan rate, peak currents during stationary or slow flow measurements would increase and could lead to higher currents than the limiting current in dual mode. Fast CV experiments are however outside the scope of this work.

Table 4. Single versus dual mode sensitivities and LOD for platinum IDEA under flow.

`	Single Mode		Dual Mode	
Flow Rate [µL/min]	Sensitivity [µA/mM]	LOD [nM]	Sensitivity [µA/mM]	LOD [nM]
0.00	1.02	63.51	6.36	10.14
11.04	1.21	53.32	6.64	9.71
52.32	1.46	44.05	6.71	9.61
116.29	1.87	34.49	6.89	9.36
203.40	2.27	28.45	**6.99**	**9.23**

4.3 MALARIA ANTIBODY IMMUNOASSAY

Off-CD

The following results are aimed at demonstrating that, while typically being quantified by an optical density measurement, ELISA can also be quantified electrochemically. Here, we first characterize the redox behavior of the TMB product that results from the assay using cyclic voltammetry. Fig. 22 shows the CV curves measured on the TMB product that resulted from the assay applied to the positive control, with and without adding stop solution. During the assay, HRP catalyzes a one electron oxidation of TMB, generating a cation free radical (ox1-TMB) that is blue and has an adsorption maximum at 653nm. Following addition of stop solution has two effects: inactivation of HRP, and further oxidation of the ox1-TMB to a diamine terminal oxidation product (ox2-TMB) that is yellow and has an adsorption maximum at 450 nm. As shown in Fig. 22, the CV curve varies whether stop solution has been added. When no stop solution is added, CV shows the two-step oxidation of TMB, with the first peak indicating the generation of ox1-TMB and the second peak the generation of ox2-TMB. When stop solution is added, ox1-TMB is not stable in the acid media and quickly turns into ox2-TMB. For this reason, in this case cyclic voltammetry generates the two-electron oxidation in one single step, and therefore only one peak is present.

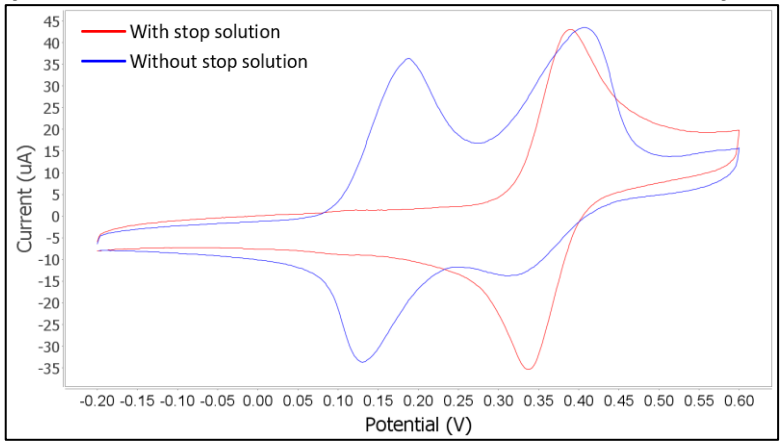

Fig. 22. CV curves obtained from a positive control adding and not adding stop solution.

Addition of stop solution is part of the standard ELISA protocol since one needs to terminate the catalytic activity of HRP at the same time in all the wells in order to lead to results that relate to the actual initial concentration of antibody and not to the incubation time of TMB with HRP. However, integration of this assay step on the disc is not possible because sulfuric acid would corrode the PMMA parts. Nevertheless, the centrifugal platform allows for accurate and timely pumping of fluids, which in this case can be used to pump out the TMB solution from the reaction chamber at specific time after the incubation with HRP has been completed. Even though the activity of HRP is not terminated, the TMB solution is no longer in contact with the enzyme and therefore the reaction is terminated.

Another aspect to consider when performing the assay on the disc is that flow of the TMB product over the electrodes can be used as demonstrated in the previous section to improve sensitivity. However, unidirectional flow as the one used in this work limits the time available for measurements. While cyclic voltammetry requires longer measuring times since the potential is scanned forward and backwards along a specific range, chronoamperometry can provide information of the content of the solution in a shorter time. In this case, chronoamperometry applies a reduction potential of -0.2V to the working electrode which causes reduction of the ox1-TMB that was generated by the HRP. Thus, by measuring the current generated by the reduction of ox1-TMB, one can quantify the concentration of ox1-TMB which relates to the concentration of antibody against Plasmodium in the initial sample.

In Fig. 23 we show the chronoamperometry curves obtained after carrying out the ELISA on the cutoff, negative and positive controls. The blank measurement was obtained from an

ELISA in which no sample was added in the first incubation step. Amplitude of the curves relates to the concentration of ox1-TMB, which is being reduced and therefore generating current. Decay of current over times arises from the expansion of the diffusion layer over the electrode, which eventually stabilizes and produces a diffusion limited steady-state current.

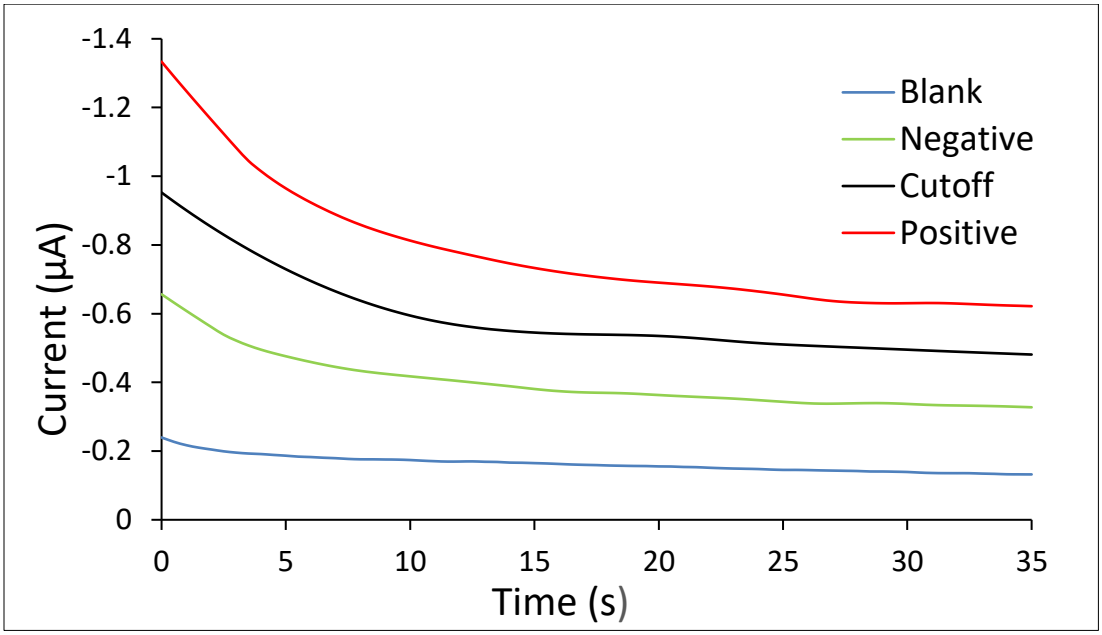

Fig. 23. Off-CD chronoamperometry curves for positive, cutoff, negative and blank. No stop solution. Working electrode at -0.2V.

On-CD

Fluidic control on the CD as required by the ELISA was first demonstrated using colored water. The spinning program and auxiliary actuation of valves using the laser succeeded in performing the fluidic operations in an effective and timely manner as shown in Fig. 24.

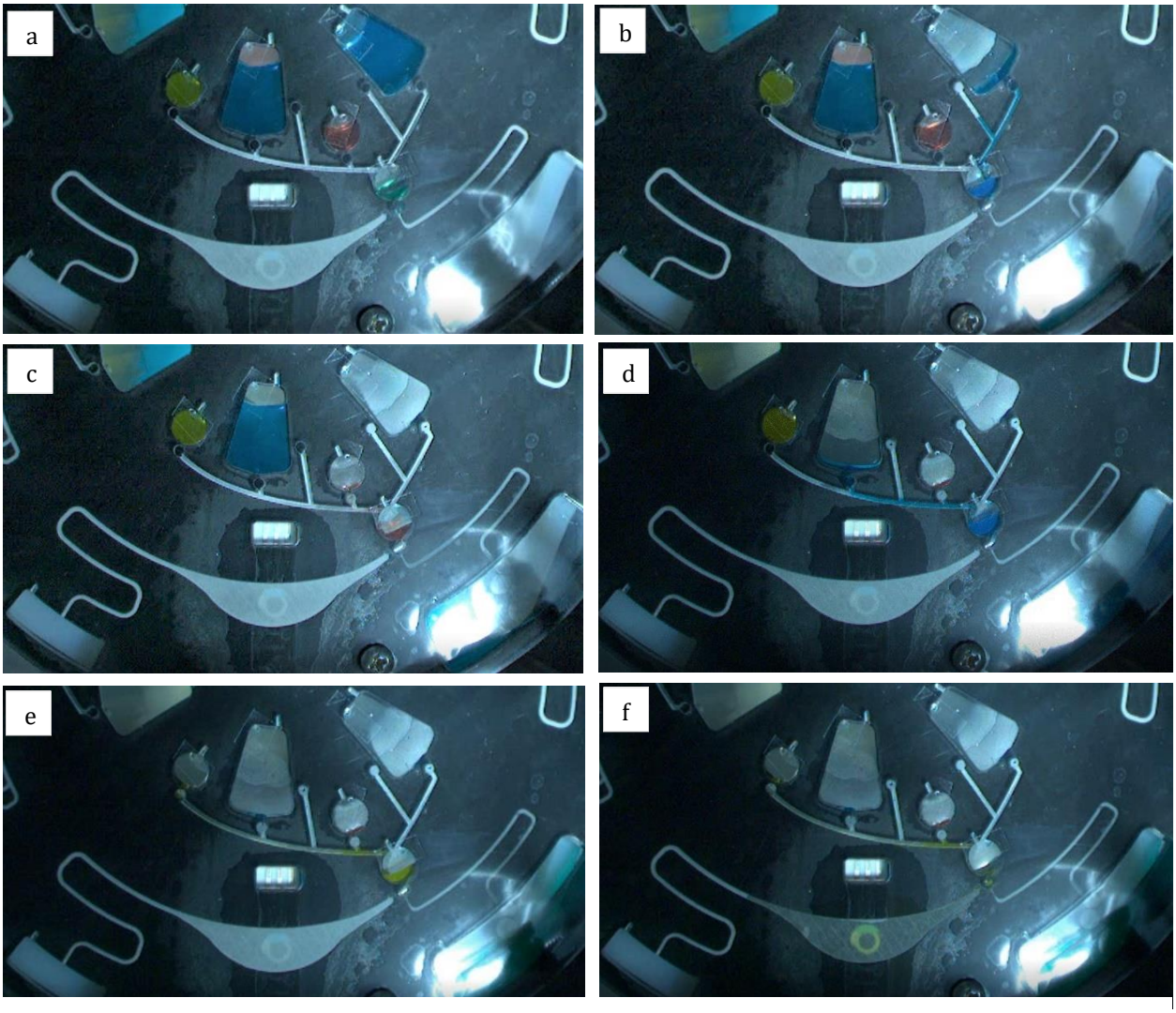

Fig. 24. Stroboscopic images of the critical operational steps. (a) Sample incubation. (b) First washing. (c) Detection antibody incubation. (d) Second washing. (e) TMB incubation. (f) Flow-enhanced detection.

General fluidic pumping from one chamber to another was continue and free of bubbles. Only minimal amounts of fluid remained in the initial chambers or in the channels. Rests of fluid remaining in their initial chambers could be totally avoided by having chambers with inclined walls, but their fabrication is not possible with laser cutting. As far as mixing, observation of the fluid in the reaction chamber while oscillating the disc demonstrated proper turbulent flows enabling effective mixing. As per the valves, active valves allowed fluid and vapor tightness and remained closed even when spinning the disc at high RPMs.

Opening using the laser had a high success rate and enabled unobstructed, continuous flow. The burst valve exiting from the reaction chamber showed a robust spin speed dependent behavior, which allowed keeping the fluid in the reaction chamber during incubation steps and flushing it out when the incubation time was over. Finally, a reproducible flow rate with a mean of 44.44µl/min is achieved over the electrodes when spinning the disc at 300RPMs. Higher flow rates could improve mass transport leading to increased currents and therefore, to improved sensitivities and LOD. However, high flow rates are not possible because, with the small amount of solution to analyze (100µl), available time to perform measurements would be greatly reduced, eventually making measurements impracticable.

In Fig. 25 we show the chronoamperometry curves obtained after carrying out the ELISA on the CD for the cutoff, negative and positive controls. A blank measurement test was also performed. As it happened in the off-CD results, the positive sample contains a greater amount of ox1-TMB which results into a higher reduction current. The decay in the current due to the expansion of the diffusion layer is also observed.

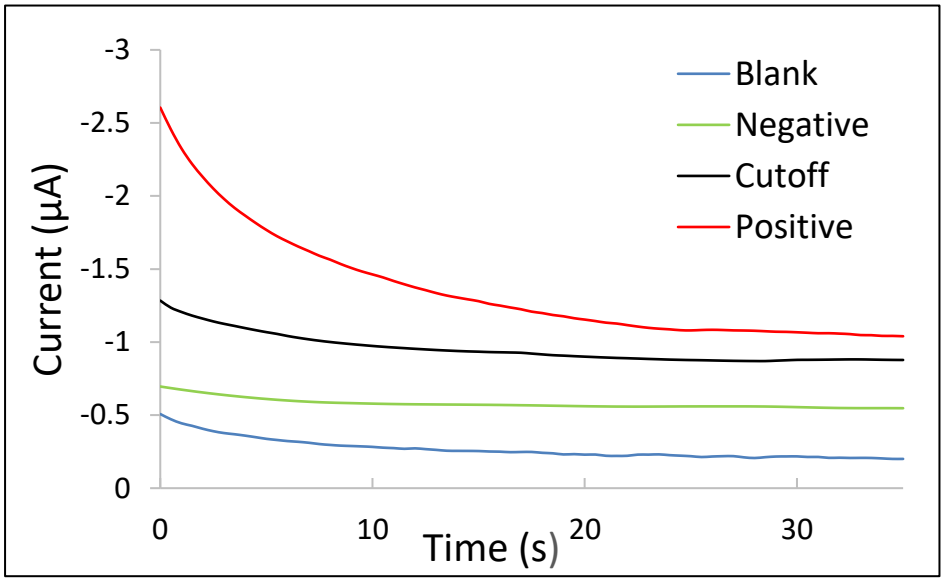

Fig. 25. Chronoamperometry curves on-CD for positive, cutoff, negative and blank. No stop solution. Working electrode at -0.2V.

Comparison

Even though the previous results indicate that electrochemical detection can be used to quantify the amount of antibody against Plasmodium, here we cannot quantitatively characterize sensor performance because only three control samples of unknown concentrations were available. Thus, a calibration curve cannot be stablished. However, a pseudo-calibration curve demonstrating qualitative detection of antibodies can be constructed using the limiting currents, as shown in Fig. 26.

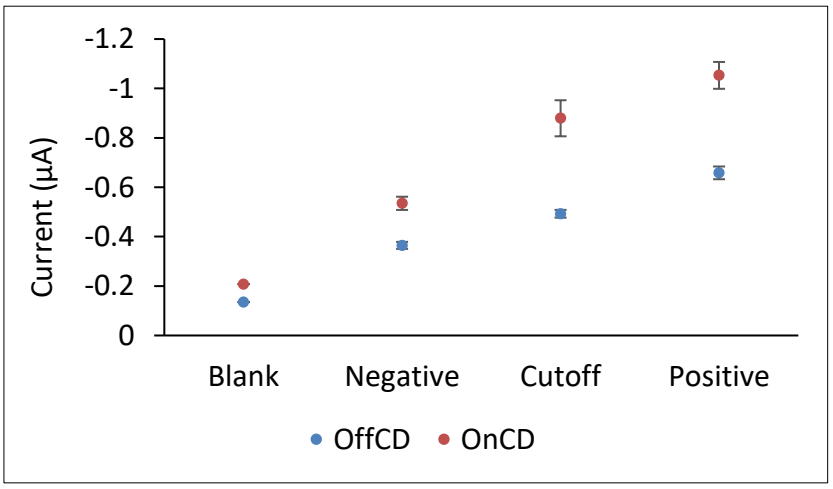

Fig. 26. Chronoamperometry limiting currents for blank, negative, cutoff and positive controls both on and off-CD. Note: error bars represent the standard deviation (n=3).

In Fig. 26. we show that performing the assay on the disc leads to significantly higher currents in comparison to the standard assay on the well plate. The cutoff value for positive determination of malaria is 0.49µA and 0.88µA for off-disc and on-disc assays respectively. This indicates that the sensitivity of the assay when performed on the CD is more than 1.5 times higher than that performed on the well plate. The increase in sensitivity is likely due to the following phenomena: flow-enhanced mass transport over the electrode surface, shorter diffusion lengths over the electrode thanks to the small channel dimensions, and increased mixing conditions during incubation steps.

5. DISCUSSION

This section discusses the methods and results of this work. Overall technical performance of the developed platform is reviewed, including an analysis of the limitations of the experimental setup and data analysis. Likewise, performance of carbon and platinum IDEAs and the effect of flow on redox amplification are discussed and contextualized. Finally, we analyze the capabilities and limitations of the platform designed to perform an automated immunoassay.

In terms of experimental setup, the main contribution of this work to the field of centrifugal microfluidics is the wireless integration of electrochemical detection on a disc, which was reported to provide a 90% decrease in noise compared to the common slip ring setup. Only a few examples of wireless systems have already been realized, and demonstration of their use for analytical applications is limited. While the current setup allows wireless data transfer, wireless powering is not available. Thus, the potentiostat needs to be removed from the centrifugal platform and connected to the power supply every time it runs out of battery. Mainly due to this battery, the potentiostat has a high weight of 0.48Kg, which affects inertia of the spinning modules and therefore negatively affecting oscillation and acceleration capability. Implementation of an inductive power transfer system or even a system harvesting energy from rotation motion could be used to wirelessly power the potentiostat, and therefore overcome the previous limitations.

Despite bypassing wiring, the use of the portable potentiostat still generates a level of noise which is mainly attributed to two sources: the noise that is inherent to the potentiostat circuitry, and the noise coming from the connection between the potentiostat and the

electrodes on the disc. We noticed that the noise had a major frequency component which was characteristic of each spinning speed. Therefore, most of the oscillatory noise, which is likely to be caused by the wired connection between the potentiostat and the electrodes, could be removed by filtering this specific frequency component during signal processing. In addition to filtering, signal processing also involved baseline selection and subtraction for each curve. The 5 points needed to create the baseline were selected manually, which limits the reproducibility of the data analysis approach.

In addition to the spinning platform with integrated electrochemical detection, the other major component of the setup is the disc. Materials and manufacturing techniques used in this work were suitable for rapid prototyping purposes, and they allowed proof of concept experiments and design optimization based on trial and error. However, limited spatial resolution of laser cutting and misalignments due to manual assembly lead to a certain level of disc-to-disc variability in terms of valve actuation. Other manufacturing techniques such as injection molding could overcome this problem and make the way towards scalable production.

The presented thesis also adds value to electrochemical detection on centrifugal microfluidics by using IDEAs, which have been reported to allow for lower LODs but have only been studied in stationary or flow injection systems. Here we demonstrated that redox cycling amplified detection can be successfully integrated on the CD and provides a more than six-fold increase in sensitivity compared to single mode measurements. Furthermore, flow-enhanced mass transport adds to redox cycling amplification, leading to a further increase in limiting currents. The use of slow flow rates enabled a maximum sensitivity of

6.99μA/mM and a LOD of 9.23nM. It must be noted that despite not impeding redox amplification, unidirectional flow of the solution over the electrodes does decrease RA and CE parameters. This is in agreement with Morita et al.[30] and Kamath et al.[11], and is explained by the fact that flow shears off redox species and affects the elliptical diffusion between bands which is the dominant factor in redox cycling for flat IDEAs. Oscillation of fluid rather than unidirectional flow could be an alternative condition to continue providing flow-enhanced mass transport while improving cycling of analytes between bands, and therefore preventing decreases in RA and CE values. However, implementation of bubble-free and high-frequency controlled oscillation on the disc would require complex pumping mechanisms such as piezoelectric transducers or microballoons. This would greatly increase complexity and cost of the disc, and that is why this option has not been considered in this work.

As far as the performance of carbon and platinum IDEAs, obtained redox amplification factors were in good agreement with previous reported use by their manufacturers Kamath et al.[11] and CH Instruments Inc respectively. Higher conductivity of platinum electrodes allowed for a lower iR drop, resulting into steeper dual mode curves compared to carbon electrodes. In carbon electrodes, iR drop compensation was needed but unavailable with the portable potentiostat, and this led to the need for broader potential scan ranges which ultimately caused a lower stability of the electrodes. Furthermore, reproducible results of carbon electrodes under the influence of flow could not be obtained due to variations in the manual alignment of the PDMS layer on the electrode. Despite these disadvantages, the established manufacturing process of carbon electrodes enables the production of 3D electrodes with heights at the scale of 1μm. Higher electrodes have a bigger surface area for

electrode exchange and allow improved diffusion between bands, leading to higher currents and redox amplification factors. Furthermore, the negative effect of flow on RA and CE parameters could be diminished in 3D carbon electrodes since the linear diffusion of redox analytes between the vertical walls (as opposed to the elliptical diffusion in flat electrodes) would be less affected by flow.

Application of the developed platform to perform an automated immunoassay was successfully demonstrated. Fully-automation was not achieved because the IR lamp for incubation and the laser for valve actuation were operated manually. However, their operation could be easily automated using a linear DC motor controlled by a programmable PCB. Moreover, manual loading of reagents and samples into their respective chambers was required before starting the assay. New dispensing fluidic systems and use of pouches storing the liquid reagents could be used to reduce manual labor. These improvements will be considered in future iterations of the current prototype. Despite these limitations, the whole assay protocol could be performed on the disc by spinning the disc as previously programmed. In total, the protocol takes around 1hour and 50 minutes to complete. This duration can slightly vary due to manual operation of the laser. The current protocol does not reduce time to results in comparison to the assay performed on the well plate, yet future optimization of mixing during incubation steps could lead to a reduction of the currently long incubation times. Another aspect to consider is that the disc prototype presented in this work is designed to be capable of analyzing human serum or plasma samples and not whole blood. In order to analyze whole blood, an additional fluidic module for blood plasma separation would be needed. This has been extensively reported in a

number of centrifugal microfluidic platforms and could be easily integrated in our disc with an additional chamber.

In addition to automation purposes, performing the ELISA on the CD has demonstrated improved electrochemical readout, mainly due to improved mixing of reagents and flow-enhanced electrochemical detection. Despite the quantitative nature of electrochemical detection, detection of antibodies against Plasmodium could only be evaluated qualitatively because only negative, cutoff and positive controls of unknown concentrations were available for testing. However, the more than 1.5-fold increase in the limiting currents measured when performing the assay on-CD versus off-CD indicates an improvement in sensitivity. A much more significant increase in sensitivity could be achieved by using IDEAs instead of the screen-printed carbon electrodes which do not allow for dual mode measurements. Our study of IDEAs properties proves the superior performance of dual mode measurements, and previous literature has reported significant improvements in sensitivity and LOD when using IDEAs to analyze the TMB product resulting from an ELISA[34]. However, the high cost of IDEAs and the need for a disposable disc to perform immunoassays led to the decision of using the cheaper screen-printed electrodes.

6. CONCLUSIONS AND FUTURE WORK

In this work, a novel fully integrated centrifugal microfluidic device capable of performing an automated enzyme-linked immunosorbent assay (ELISA) has been developed. The system consists of a central platform with centrifugal and readout functions, and a polymer-based microfluidic disc for fluidic handling and sensing. In addition to a DC motor for rotary actuation of the disc, the central platform includes a portable potentiostat that controls and measures potentials and currents at the electrodes that are integrated in the disc, and transfers data via Bluetooth to a stationary computer. This instrumentation allows for wireless electrochemical detection, which was reported to provide on-line, continuous measurements while the disc was spinning at reduced noise levels of 1.84μA compared to 19.09μA in the conventional wired setup. As far as the sensing electrodes, carbon and platinum IDEAs were integrated on the disc and their performance was characterized using ferri-ferrocyanide redox couple. While carbon IDEAs led to higher currents and redox amplification factors, platinum IDEAs showed to be more stable throughout experiments and had less iR drop. Hydrodynamic properties of platinum IDEAs were studied and indicated that improved sensor performance is achieved when taking measurements in dual mode and while imposing slow flow rates over the electrode surface. At a flow rate of 203.4μl/min, we achieved an improved sensitivity of 6.99μA/mM leading to a LOD of 9.23nM.

The previously demonstrated wireless, flow-enhanced electrochemical detection was used on a disc designed to perform an ELISA. The disc includes single shot laser valves that allow for robust and reliable fluidic control, which is required to perform the multiple-step assay.

After capturing the target antibody from the sample and carrying out the following assay steps, electrochemical detection using screen-printed circular carbon electrodes is performed. As a model system, antibody against Plasmodium, a marker of malaria, was used as the target biomolecule for detection. The platform showed to successfully automate the otherwise labor-intense immunoassay and demonstrated an improved electrochemical detection thanks to enhanced mixing conditions and flow-enhanced mass transport.

The next iteration of the current disc performing the immunoassay should work towards the use of carbon IDEAs. Unlike the screen-printed circular electrodes that were used here to show proof-of-concept, carbon IDEAs would provide the possibility for dual mode measurements and therefore, lead to a lower LOD. Due to the need for a disposable disc, the cheaper cost of carbon IDEAs makes them to be more suitable for this application than platinum IDEAs. Furthermore, implementation of fluidic conditions other than unidirectional flow, such as reciprocating or oscillating flows, could add value in two aspects: time available for measurements would be longer, and redox cycling between adjacent bands could be improved leading to higher amplification factors.

Finally, and more as longer-term goals, efforts should be made to translate the current prototype into a POCT system, focusing on their portability, usability and short time-to-results qualities. This would require designing a more compact platform with simpler and smaller hardware and a central controller with a user-friendly interface. Optimization of the assay should be carried out to minimize time-to-results, and a sample preparation unit should be added to the disc in order to allow a complete sample-to-answer analysis from whole blood.

7. REFERENCES

1. Tang, M., Wang, G., Kong, S. K. & Ho, H. P. A review of biomedical centrifugal microfluidic platforms. *Micromachines* **7**, (2016).

2. Lee, B. S. *et al.* Fully integrated lab-on-a-disc for simultaneous analysis of biochemistry and immunoassay from whole blood. *Lab Chip* **11**, 70–78 (2011).

3. Kettler, H., White, K. & Hawkes, S. Mapping the landscape of diagnostics for sexually transmitted infections: Key findings and recommandations. *Unicef/Undp/World Bank/Who* 1–44 (2004). doi:WHO reference number: TDR/STI/IDE/04.1

4. Morelli, L. *et al.* Injection molded lab-on-a-disc platform for screening of genetically modified *E. coli* using liquid–liquid extraction and surface enhanced Raman scattering. *Lab Chip* **18**, 869–877 (2018).

5. Kong, L. X., Perebikovsky, A., Moebius, J., Kulinsky, L. & Madou, M. Lab-on-a-CD: A Fully Integrated Molecular Diagnostic System. *J. Lab. Autom.* **21**, 323–355 (2016).

6. Lutz, S. *et al.* Microfluidic lab-on-a-foil for nucleic acid analysis based on isothermal recombinase polymerase amplification (RPA). *Lab Chip* **10**, 887–893 (2010).

7. Delgado, S. M. T., Kinahan, D. J., Kilcawley, N. A. & Julius, L. A. N. A Fully Automated Wirelessly Powered Centrifugal Platform Towards a Sample-To-Answer Chemiluminescent Elisa Assay for Cvd Detection. *Mtas 2016* 1348–1349 (2016).

8. Zainal, M. A., Yunos, Y. M., Rahim, R. A. & Mohamed Ali, M. S. Wireless valving for centrifugal microfluidic disc. *J. Microelectromechanical Syst.* **26**, 1327–1334 (2017).

9. Burger, R., Amato, L. & Boisen, A. Detection methods for centrifugal microfluidic platforms. *Biosens. Bioelectron.* **76**, 54–67 (2016).

10. Gilmore, J., Islam, M. & Martinez-Duarte, R. Challenges in the use of compact disc-based centrifugal microfluidics for healthcare diagnostics at the extreme point of care. *Micromachines* **7**, (2016).

11. Kamath, R. Three-Dimensional Carbon Interdigitated Electrode Arrays for Redox-Amplification. *Analytical Chemistry.* **86**, 2963-2971 (2014).

12. Lee, B. S. *et al.* A fully automated immunoassay from whole blood on a disc. *Lab Chip* **9**, 1548–1555 (2009).

13. Madou, M. J. Recent advances in the development of micropumps , microvalves and micromixers and the integration of carbon electrodes on centrifugal microfluidic platforms Mohammad Mahdi Aeinehvand , Fatimah Ibrahim *, Wisam Al-Faqheri and Karunan Joseph. **15**, (2018).

14. Lai, S. *et al.* Design of a Compact Disk-like Microfluidic Platform for Enzyme-Linked Immunosorbent Assay. *Anal. Chem.* **76**, 1832–1837 (2004).

15. Park, J. M., Cho, Y. K., Lee, B. S., Lee, J. G. & Ko, C. Multifunctional microvalves control by optical illumination on nanoheaters and its application in centrifugal microfluidic devices. *Lab Chip* **7**, 557–564 (2007).

16. Garcia-Cordero, J. L. *et al.* Optically addressable single-use microfluidic valves by laser printer lithography. *Lab Chip* **10**, 2680–2687 (2010).

17. Abi-Samra, K. *et al.* Thermo-pneumatic pumping in centrifugal microfluidic platforms. *Microfluid. Nanofluidics* **11**, 643–652 (2011).

18. Noroozi, Z., Kido, H. & Madou, M. J. Electrolysis-Induced Pneumatic Pressure for Control of Liquids in a Centrifugal System. *J. Electrochem. Soc.* **158**, P130 (2011).

19. Haeberle, S., Schmitt, N., Zengerle, R. & Ducrée, J. Centrifugo-magnetic pump for gas-to-liquid sampling. *Sensors Actuators, A Phys.* **135**, 28–33 (2007).

20. Gorkin, R. *et al.* Centrifugo-pneumatic valving utilizing dissolvable films. *Lab Chip* **12**, 2894–2902 (2012).

21. Byrnes, S. A. & Weigl, B. H. Selecting analytical biomarkers for diagnostic applications: a first principles approach. *Expert Rev. Mol. Diagn.* **18**, 19–26 (2018).

22. Grieshaber, D., MacKenzie, R., Vörös, J. & Reimhult, E. Electrochemical Biosensors - Sensor Principles and Architectures. *Sensors (Basel)* **8**, 1400–1458 (2008).

23. Faulkner, L. R., Bard, A. J. Electrochemical Methods: Fundamentals and Applications. (2001).

24. Interdigitated Electrode Arrays (IDEAs). White paper by UCI BioMEMS group.

25. Dam, V. A. T., Olthuis, W. & Van Den Berg, A. Redox cycling with facing interdigitated array electrodes as a method for selective detection of redox species. *Analyst* **132**, 365–370 (2007).

26. Odijk, M., Straver, M., Olthuis, W. & Berg, A. Van Den. Microfluidic Sensor for Ultra High Redox Cycling Amplification for Highly Selective Electrochemical Measurements. *Sensors (Peterborough, NH)* 1281–1283 (2011). doi:10.2196/jmir.3802\r10.1590/1678-775720140339

27. Torres Delgado, S. M., Korvink, J. G. & Mager, D. The eLoaD platform endows centrifugal microfluidics with on-disc power and communication. *Biosens. Bioelectron.* **117**, 464–473 (2018).

28. Kim, T. H. *et al.* Flow-enhanced electrochemical immunosensors on centrifugal microfluidic platforms. *Lab Chip* **13**, 3747–3754 (2013).

29. Andreasen, S. Z. *et al.* Integrating electrochemical detection with centrifugal microfluidics for real-time and fully automated sample testing. *RSC Adv.* **5**, 17187–17193 (2015).

30. Morita, M., Niwa, O. & Horiuchi, T. *Interdigitated array microelectrodes as electrochemical sensors*. *Electrochimica Ado* **42**, (1997).

31. Aoki, K. Approximate models of interdigitated array electrodes for evaluating steady-state currents. *J. Electroanal. Chem.* **284**, 35–42 (1990).

32. Konopka, S. J., McDuffie, B., Arvia, A. J., Bazan, J. C. & W Carrozza, J. S. *Polarographic Techniques*. *J. Amer. Chem. Soc* **10**, (1929).

33. Goldstein, E. L. & Van de Mark, M. R. Electrode cleaning and anion effects on ksfor K3Fe(CN)6couple. *Electrochim. Acta* **27**, 1079–1085 (1982).

34. Lee, G. Y. *et al.* Redox cycling-based immunoassay for detection of carcinogenic embryonic antigen. *Anal. Chim. Acta* **971**, 33–39 (2017).